NSTX-U

Supported by U.S. DEPARTMENT OF ENERGY Office of Science

Pedestal Structure, Fluctuations, and Transport Analysis during an ELM cycle on NSTX

Ahmed Diallo[1]

R. Maingi[2], D. Smith[3], G. Kramer[1], S. Kubota[4], T. Osborne[5], J. Canik[2], S-H Ku[1], M. Podesta[1], W. Guttenfelder[1], R. Bell[1], B. LeBlanc[1], C-S. Chang[1] and the NSTX Research Team

[1] PPPL
[2] ORNL
[3] University Wisconsin
[4] UCLA
[5] GA

TTF-Workshop
Annapolis, MD
April 2012

Coll of Wm & Mary
Columbia U
CompX
General Atomics
FIU
INL
Johns Hopkins U
LANL
LLNL
Lodestar
MIT
Lehigh U
Nova Photonics
Old Dominion
ORNL
PPPL
Princeton U
Purdue U
SNL
Think Tank, Inc.
UC Davis
UC Irvine
UCLA
UCSD
U Colorado
U Illinois
U Maryland
U Rochester
U Tennessee
U Tulsa
U Washington
U Wisconsin
X Science LLC

Culham Sci Ctr
York U
Chubu U
Fukui U
Hiroshima U
Hyogo U
Kyoto U
Kyushu U
Kyushu Tokai U
NIFS
Niigata U
U Tokyo
JAEA
Inst for Nucl Res, Kiev
Ioffe Inst
TRINITI
Chonbuk Natl U
NFRI
KAIST
POSTECH
Seoul Natl U
ASIPP
CIEMAT
FOM Inst DIFFER
ENEA, Frascati
CEA, Cadarache
IPP, Jülich
IPP, Garching
ASCR, Czech Rep

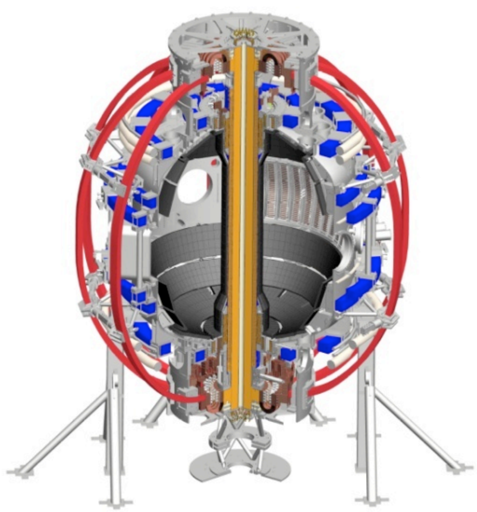

Characterize the pedestal structure evolutions and pedestal region turbulence to elucidate the role of transport in pedestal constraints

- Summary of the pedestal structure characterization in ELMy H-modes

- Interpretive transport analysis
  - SOLPS calculations
  - Comparison with XGC0 - neoclassical simulations

- Fluctuations characterizations during the inter-ELM phase

- Preliminary δf XGC1 calculations and comparison with observations

- Analysis of lithium effects on transport and turbulence will be shown in this afternoon session by D. Boyle; R. Maingi

Dedicated experiments to vary the pedestal pressure height and width through I_p scans were performed on NSTX

- Constant injected power (P_{NBI}) and magnetic field (B_T)
- Lower single null slightly downward and fixed high triangularity shaping.

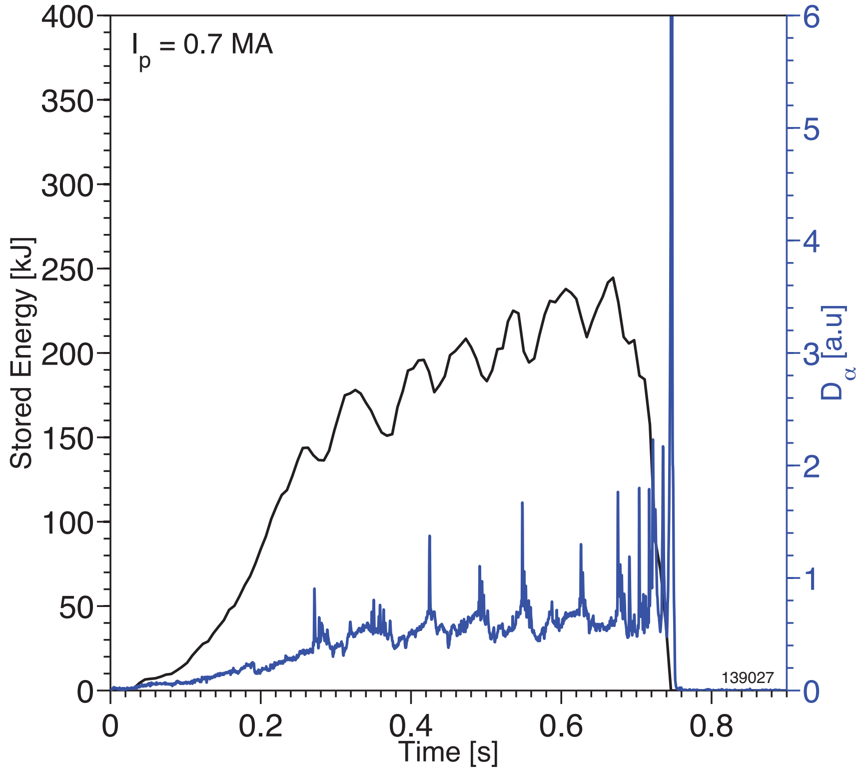

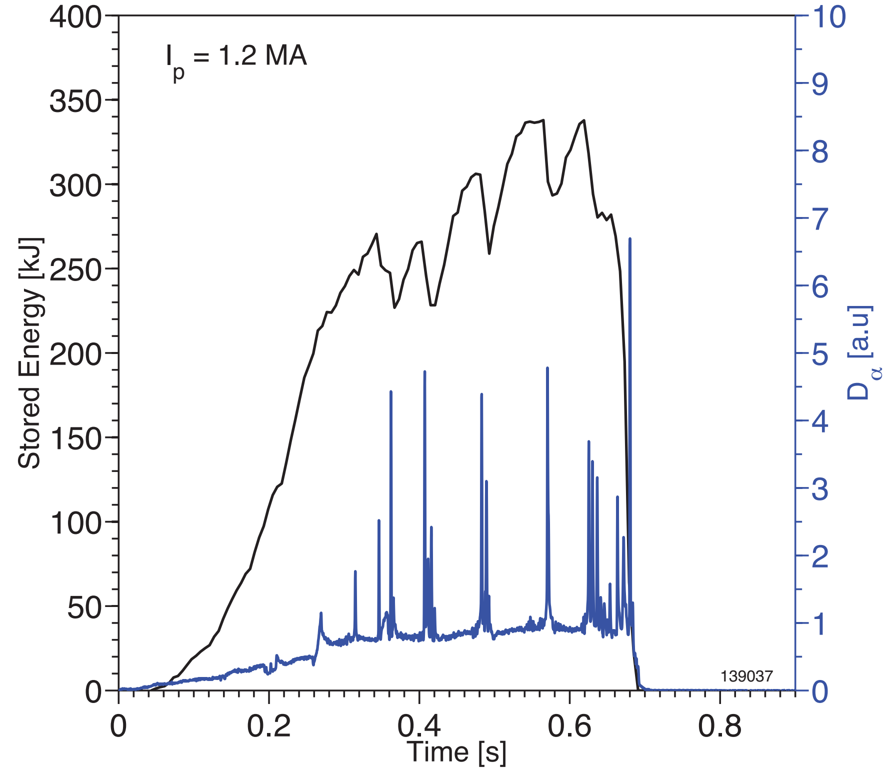

- Large drop (up to 15%) of stored energy (W_{mhd}) after each ELM crash.
  - Pedestal stored energy ~ 25% - 40% of W_{mhd}
- Implicitly generating scans of the pedestal structure.

Radial profiles of density, temperature and pressure are composite of times between multiple fraction of ELMs

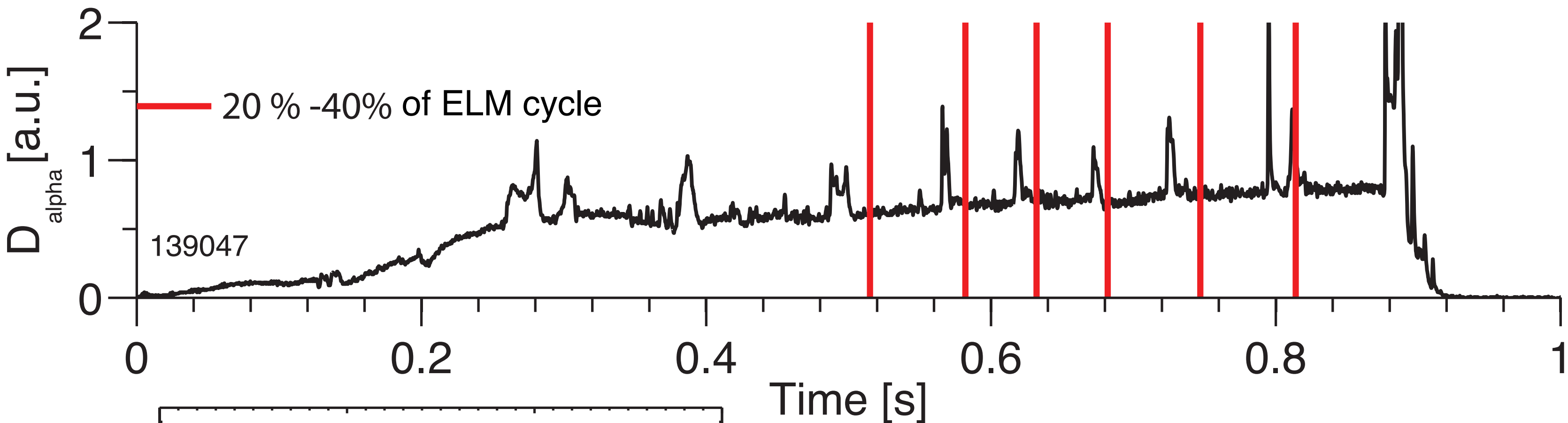

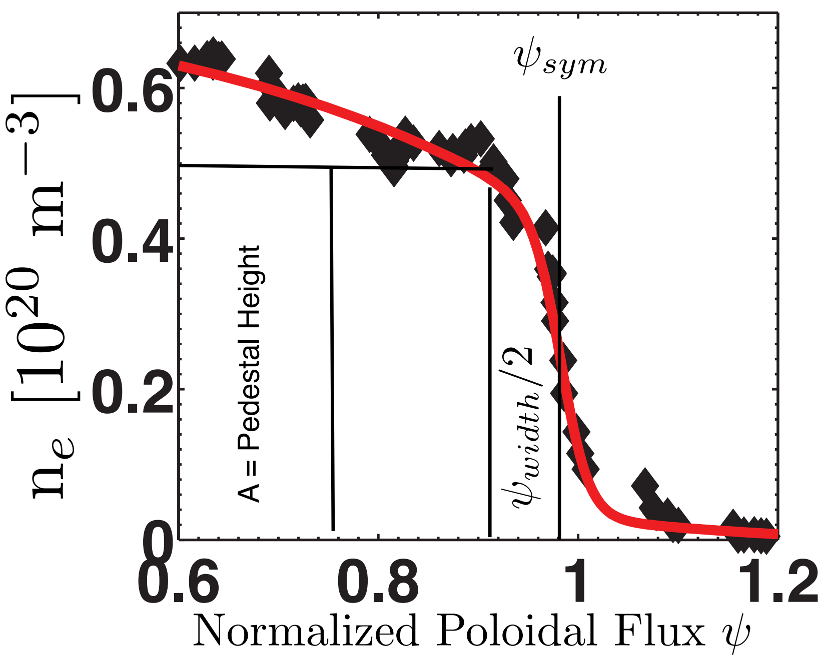

- Electrons edge radial profiles are fitted using a modified tanh function

$$N(\psi) = A \tanh\left(\frac{\psi_{sym} - \psi}{\psi_{width}}\right) + offset$$

R. Groebner and T. Osborne PoP (1998)

- Ion profiles are spline fitted

Temperature pedestal height increases during the ELM cycle while the density pedestal show no convincing trend

- More than a factor of two increase in pedestal temperature
- Density pedestal is much less sensitive to the ELM cycle
- Heat and particle evolutions appear to be decoupled

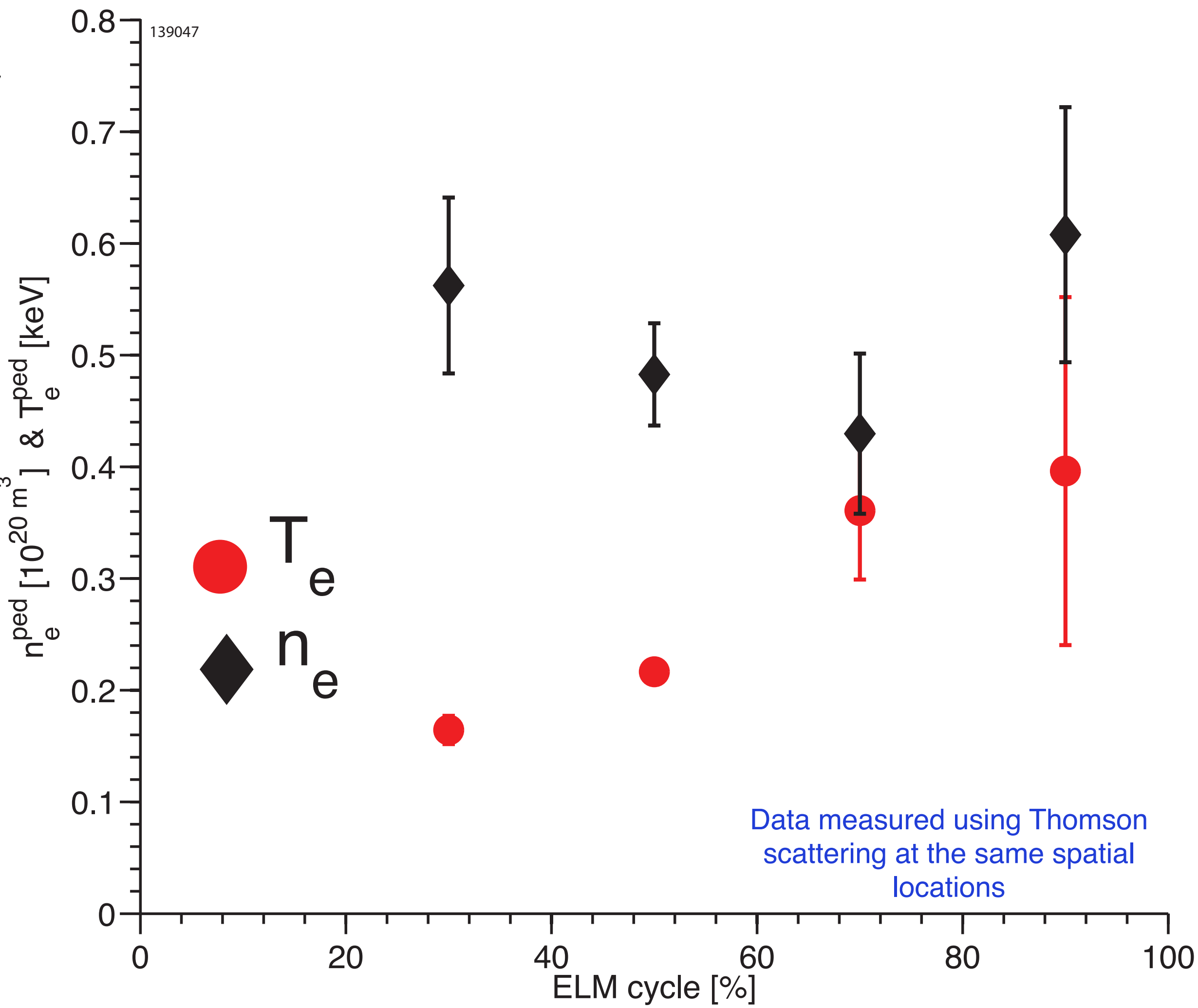

Pedestal width and height progressively increase during ELM cycle but the peak pressure gradient remains clamped

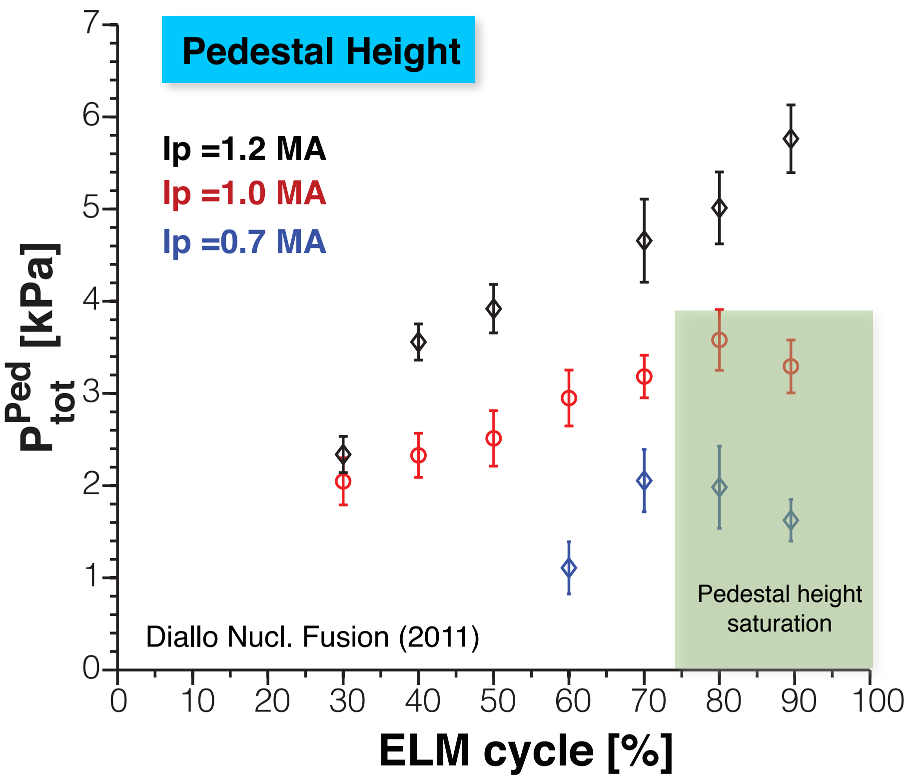

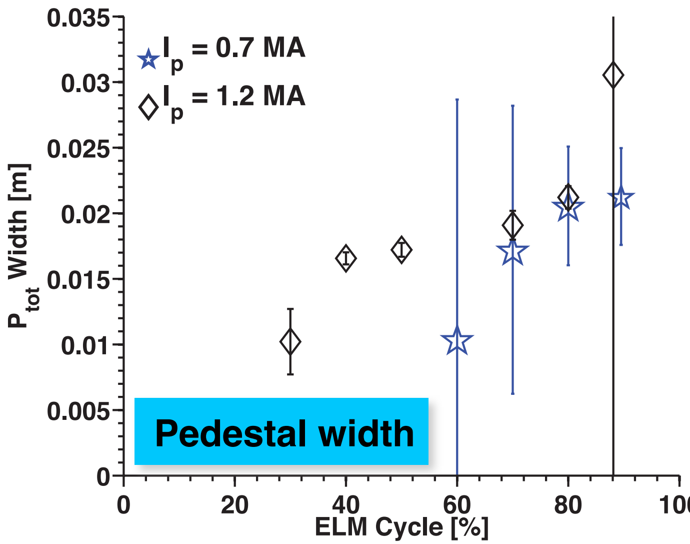

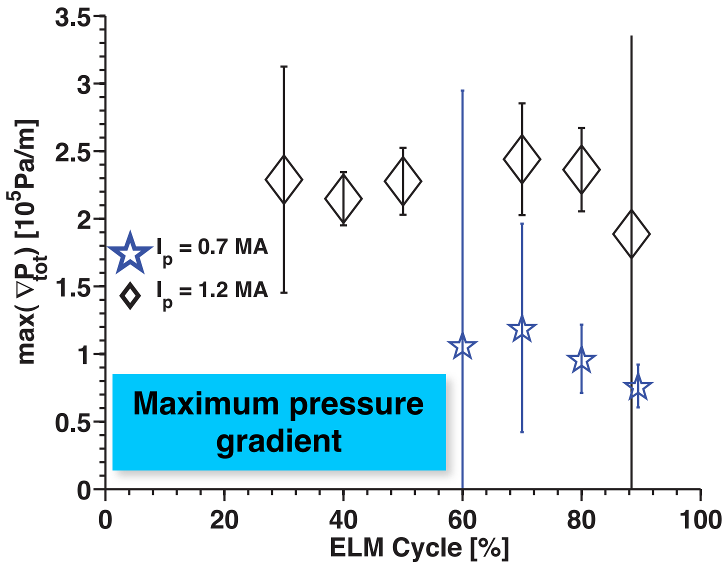

- Pedestal height increases by a factor ≤ 3
  - Height scales with I_p
- Pedestal width increases independently of I_p
- Gradient is clamped early in ELM cycle

Measured pedestal pressure width scales with $\sqrt{\beta_\theta}$

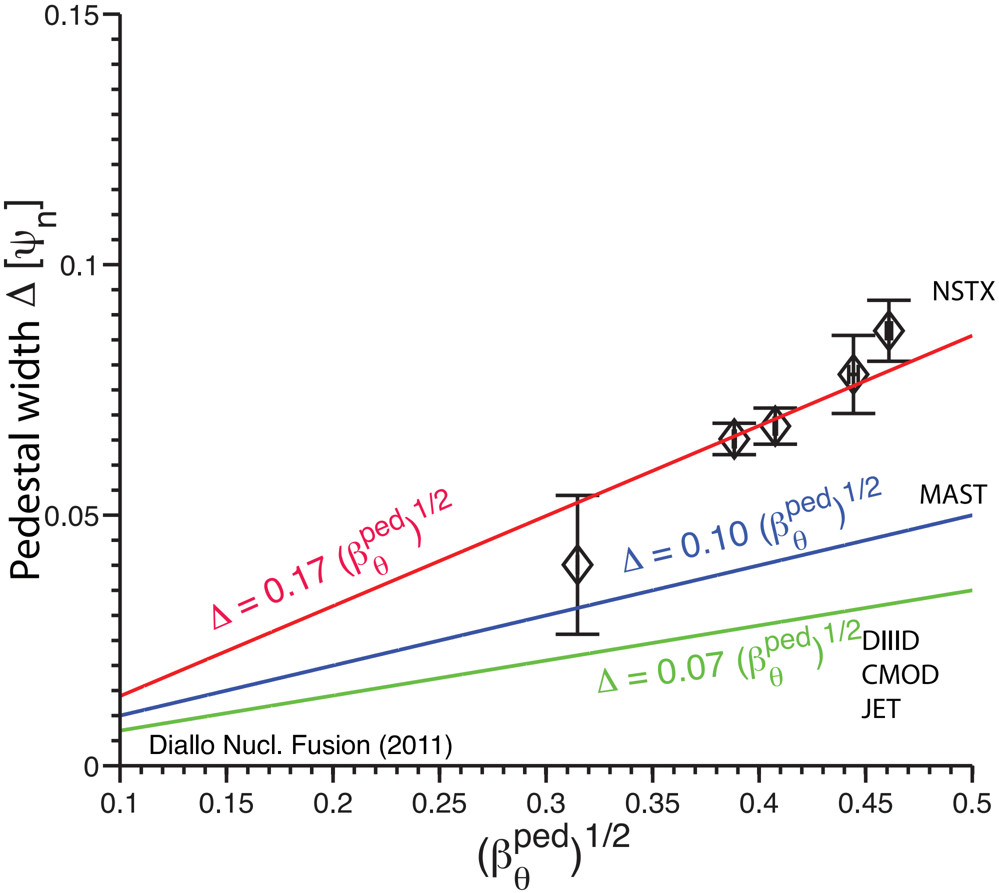

$$\beta_\theta^{ped} = 2\mu_0 P_{ped}/B_\theta^2$$

- Good description of the width scaling over multiple machines (DIIID, CMOD, JET, MAST)

Groebner, NF, (2009)
Kirk, PPCF, (2009)
Beurkens, PoP, (2011)
Walk, to be published, Nucl. Fusion (2012)

- In NSTX, the observed width is larger than conventional tokamaks
  - NSTX pedestal width is 1.7 and 2.4 larger than MAST and DIII-D respectively

- Larger width in NSTX could sustain significant edge current

Saturation of the gradient is ubiquitous across devices, but different trends in pedestal height evolution are observed

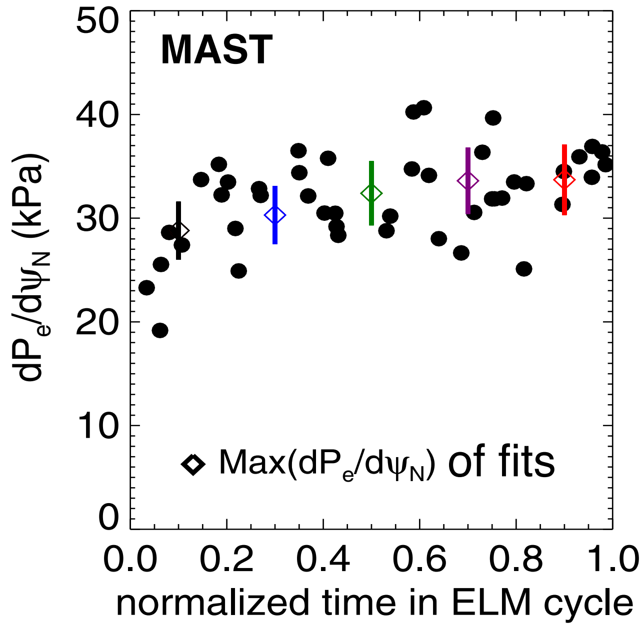

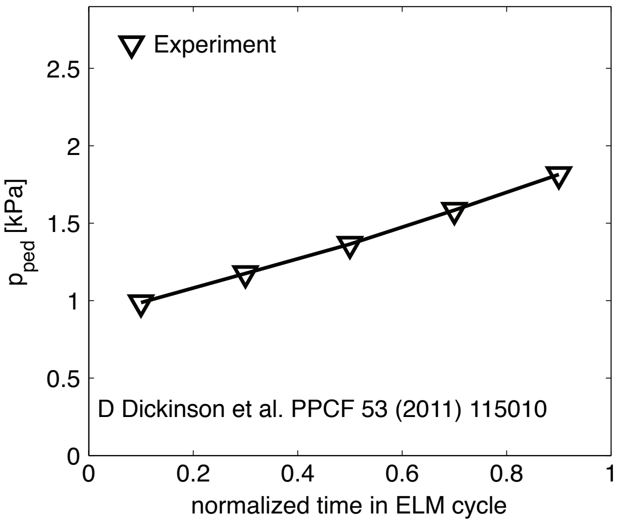

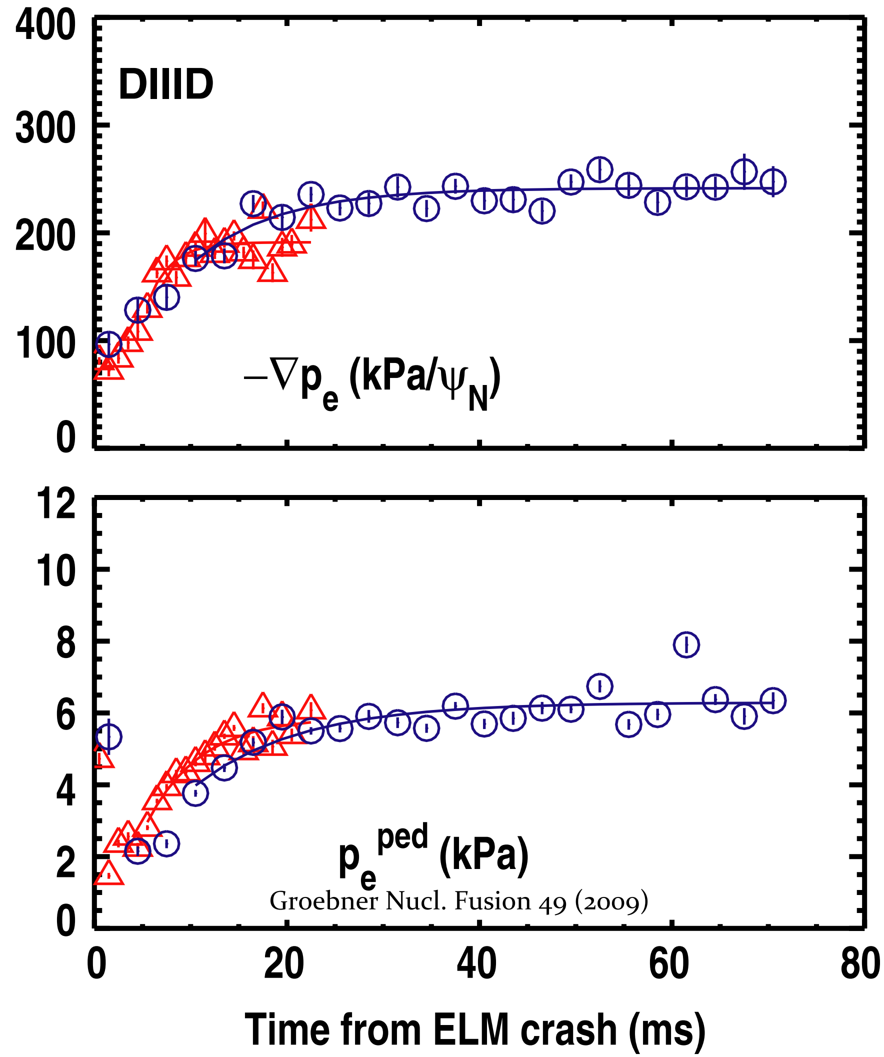

Characterize the pedestal structure evolutions and pedestal turbulence to elucidate the role of transport setting the pedestal structure

- Summary of the Pedestal structure characterization in ELMy H-modes
- Interpretive Transport Analysis
  - SOLPS calculations
  - Comparison with XGC0 - neoclassical simulations
- Fluctuations characterizations during the inter-ELM phase
- Preliminary δf XGC1 calculations and comparison with observations
- Summary/Discussion

2D SOLPS* modeling shows modest variations of the transport coefficients at the pedestal top

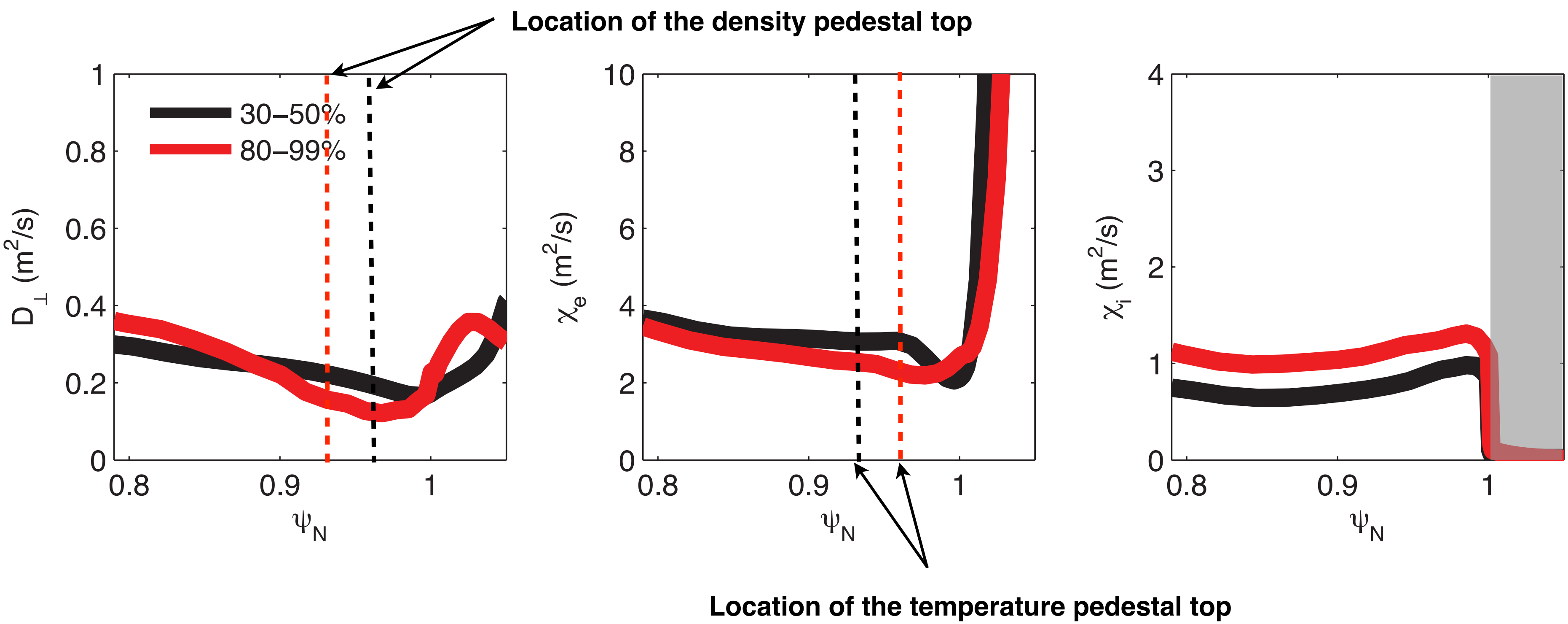

- Particle flux at the pedestal top is insignificant during the inter-ELM
- No clear trend for the electron heat flux
- Ion heat flux becomes larger later in the ELM cycle

*R. Schneider et al, Contrib. Plasma Phys. 46 (2006)

Ion heat diffusivity comparison: SOLPS and XGC0

XGC0 computes the neoclassical transport parameters

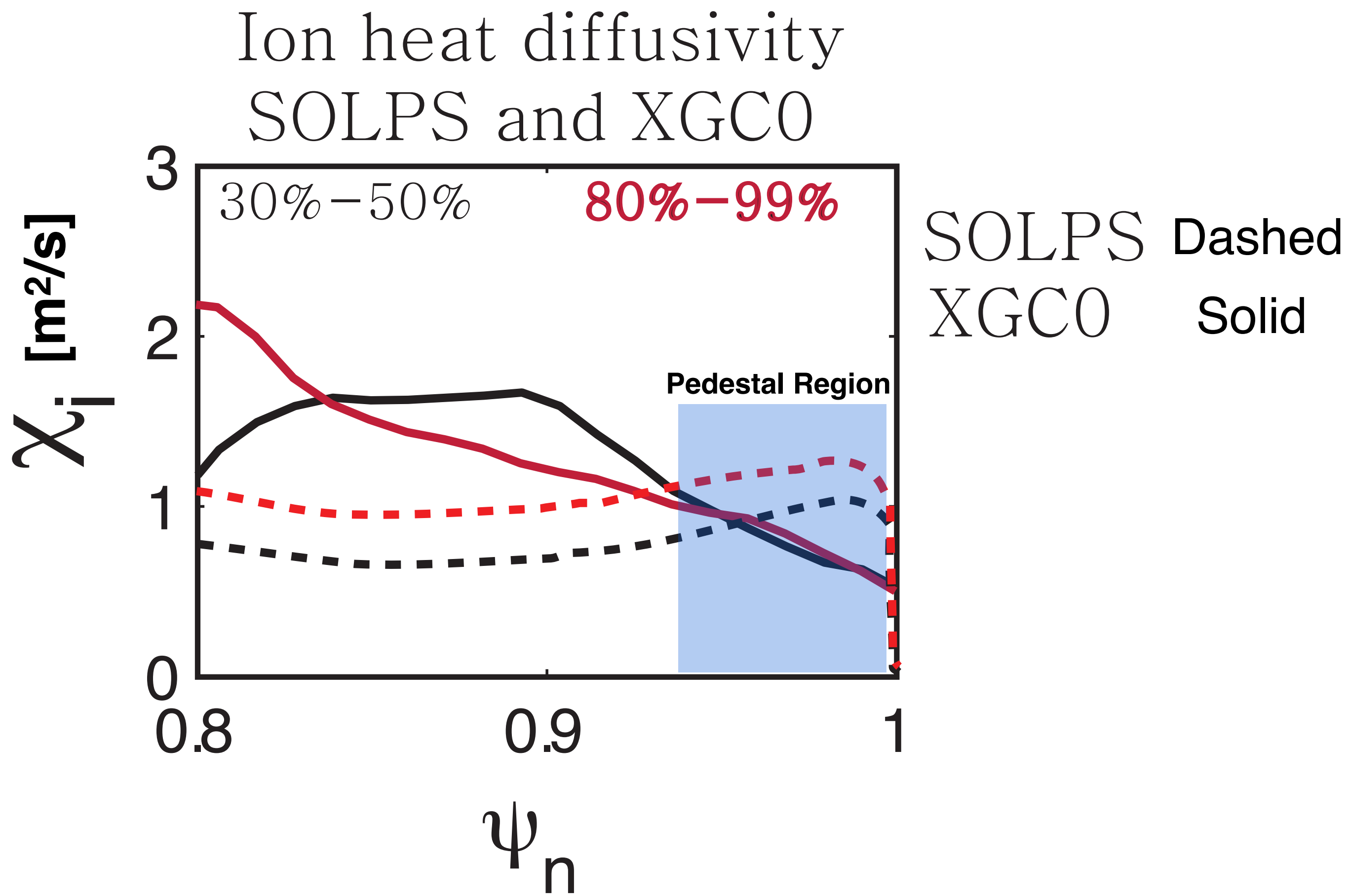

- Neoclassical ion diffusivity remains unchanged during the inter-ELM phase in the pedestal region
- In the pedestal region SOLPS shows larger than neoclassical ion diffusivity

Characterize the pedestal structure evolutions and pedestal turbulence to elucidate the role of transport setting the pedestal structure

- Summary of the Pedestal structure characterization in ELMy H-modes
- Interpretive Transport Analysis
  - SOLPS calculations
  - Comparison with XGC0 - neoclassical simulations
- Fluctuations characterizations during the inter-ELM phase
- Preliminary δf XGC1 calculations and comparison with observations
- Summary/Discussion

BES yields measurements of the poloidal correlation at the density pedestal top

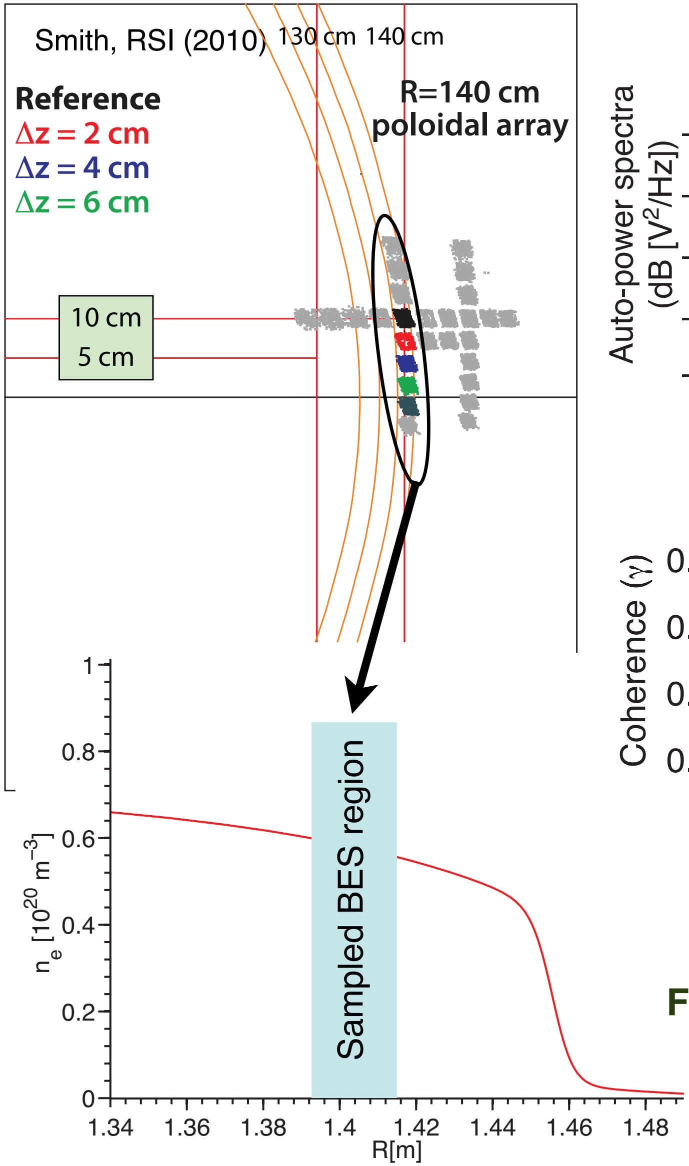

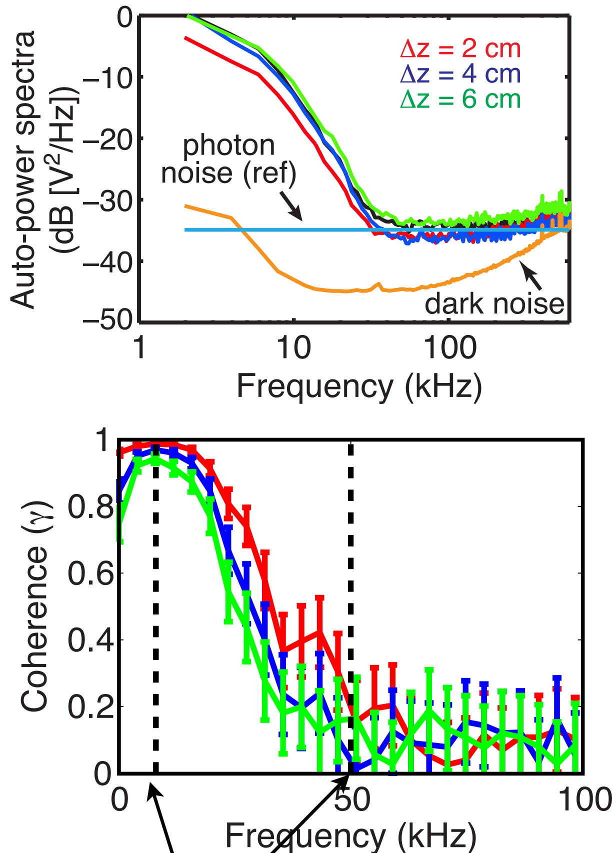

Frequency range of interest

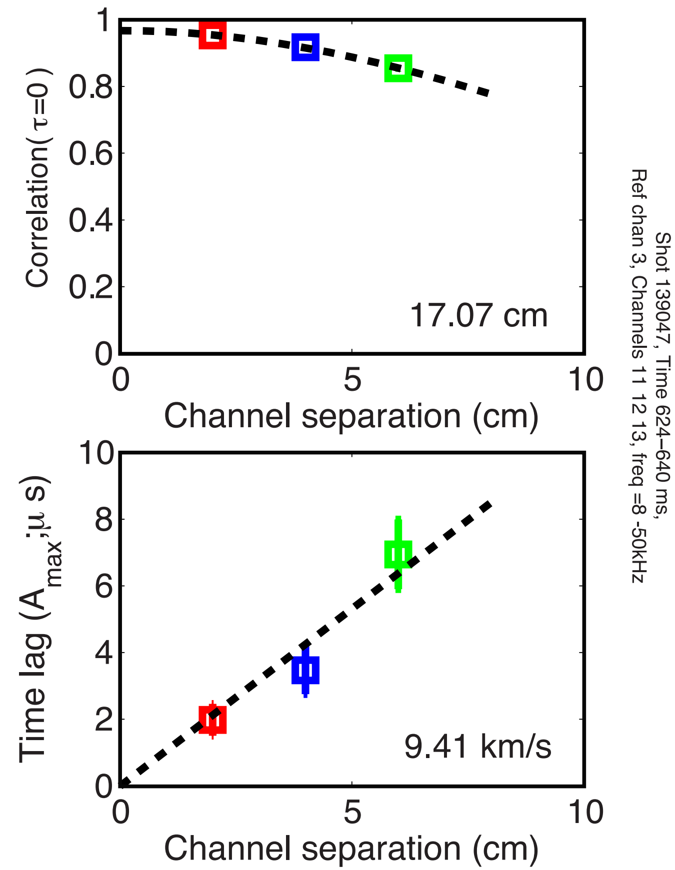

D. Smith: this meeting

BES provides measurements of the poloidal correlation length and poloidal velocity

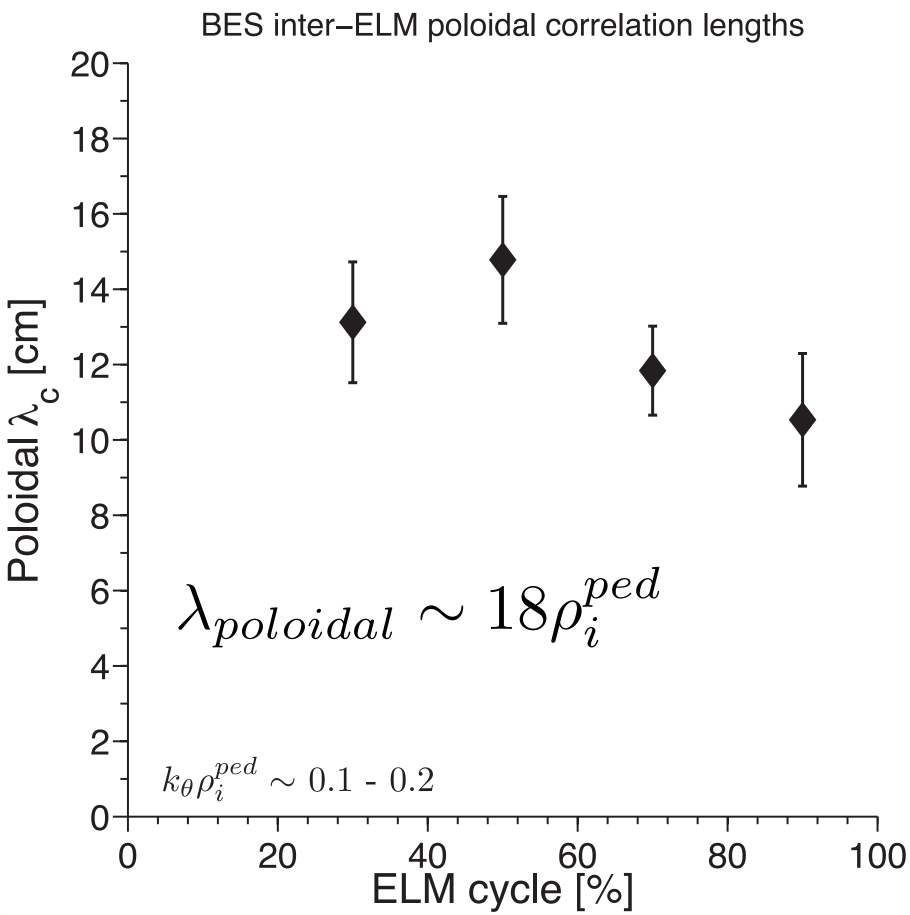

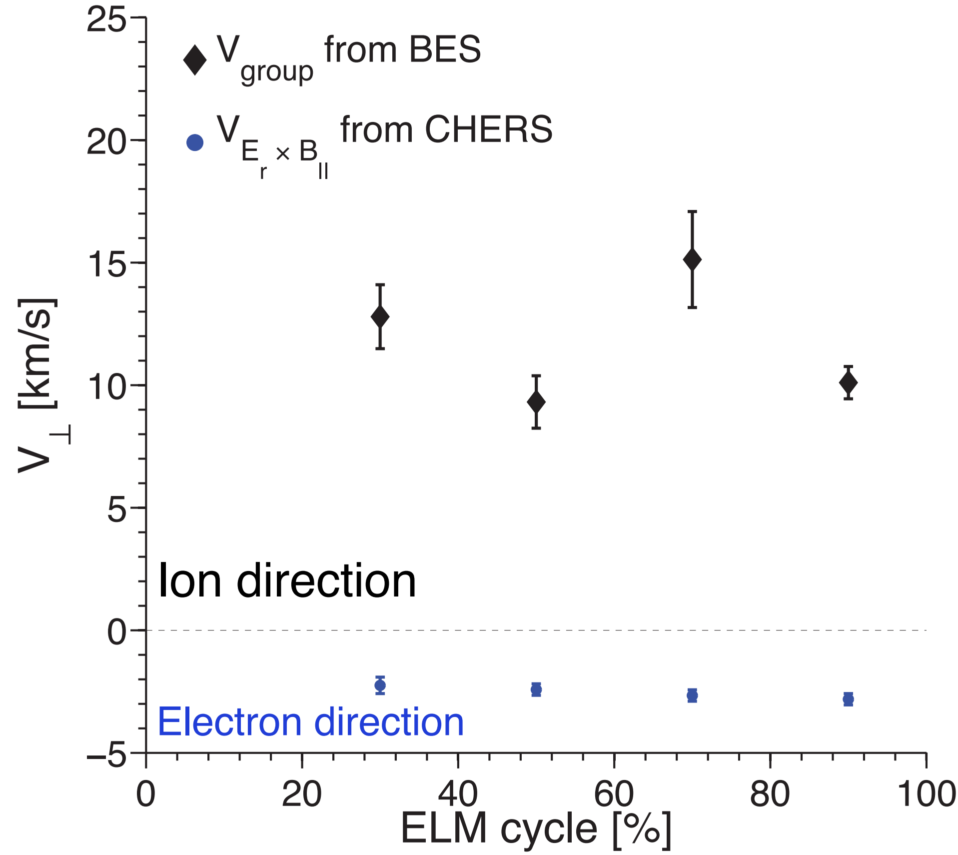

- Modest change in poloidal correlation length during the inter-ELM phase
  - Poloidal correlation length corresponds to toroidal mode number (rk_θ/q) n = 2 - 3
- Measurements show ion scale fluctuation in the pedestal top

Evolution of the radial displacement power spectra indicates an increase of the fluctuation level during the last 40% of ELM cycle

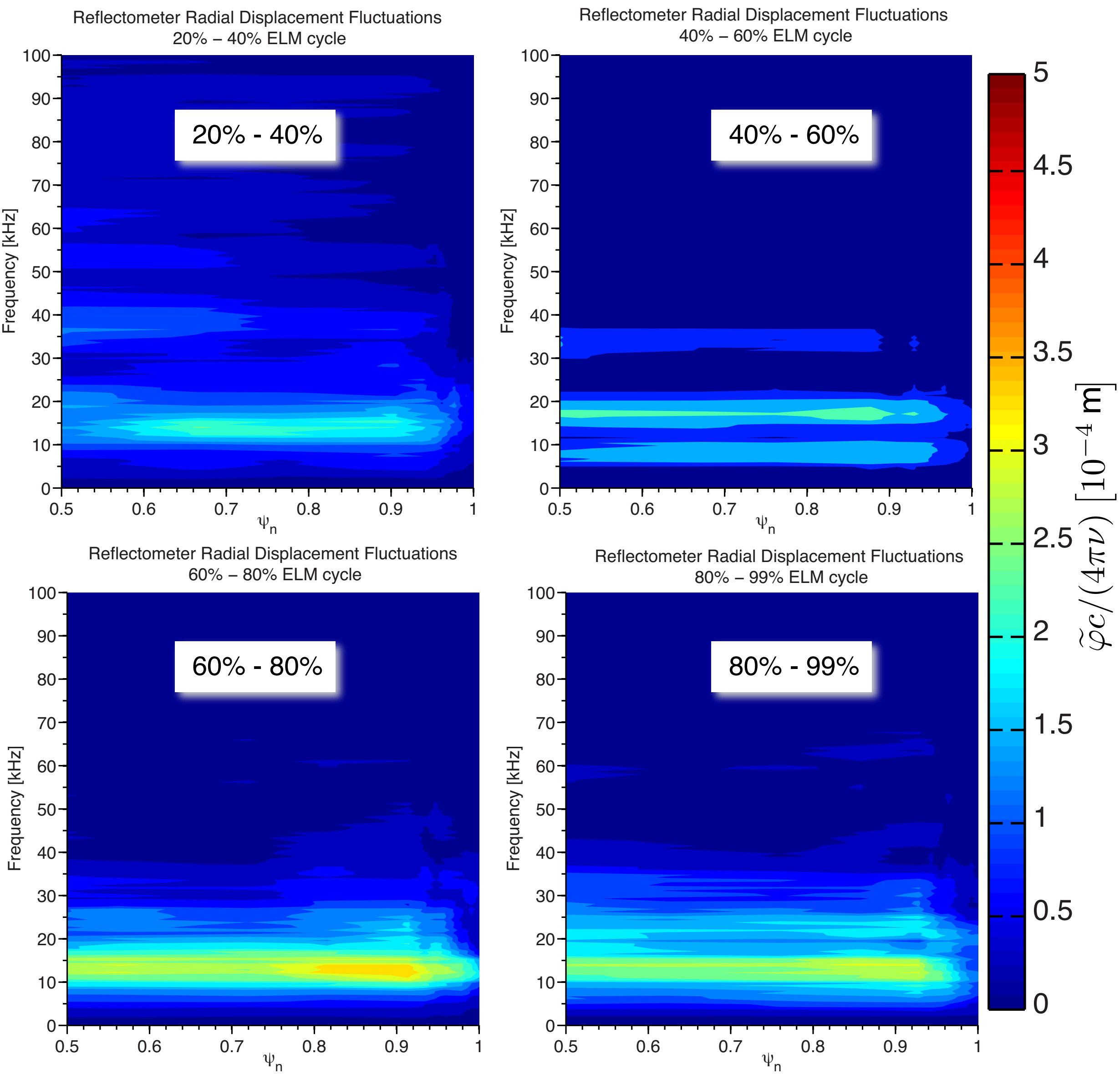

- Radial displacement induced by fluctuations
  - Existence of broadband fluctuations centered around 12 kHz
- Increase of the overall mode amplitude late in ELM cycle
- Caution: Localization of the mode is difficult to assess as it could be due the density scale length

Evolution of the radial displacement power spectra indicates an increase of the fluctuation level during the last 40% of ELM cycle

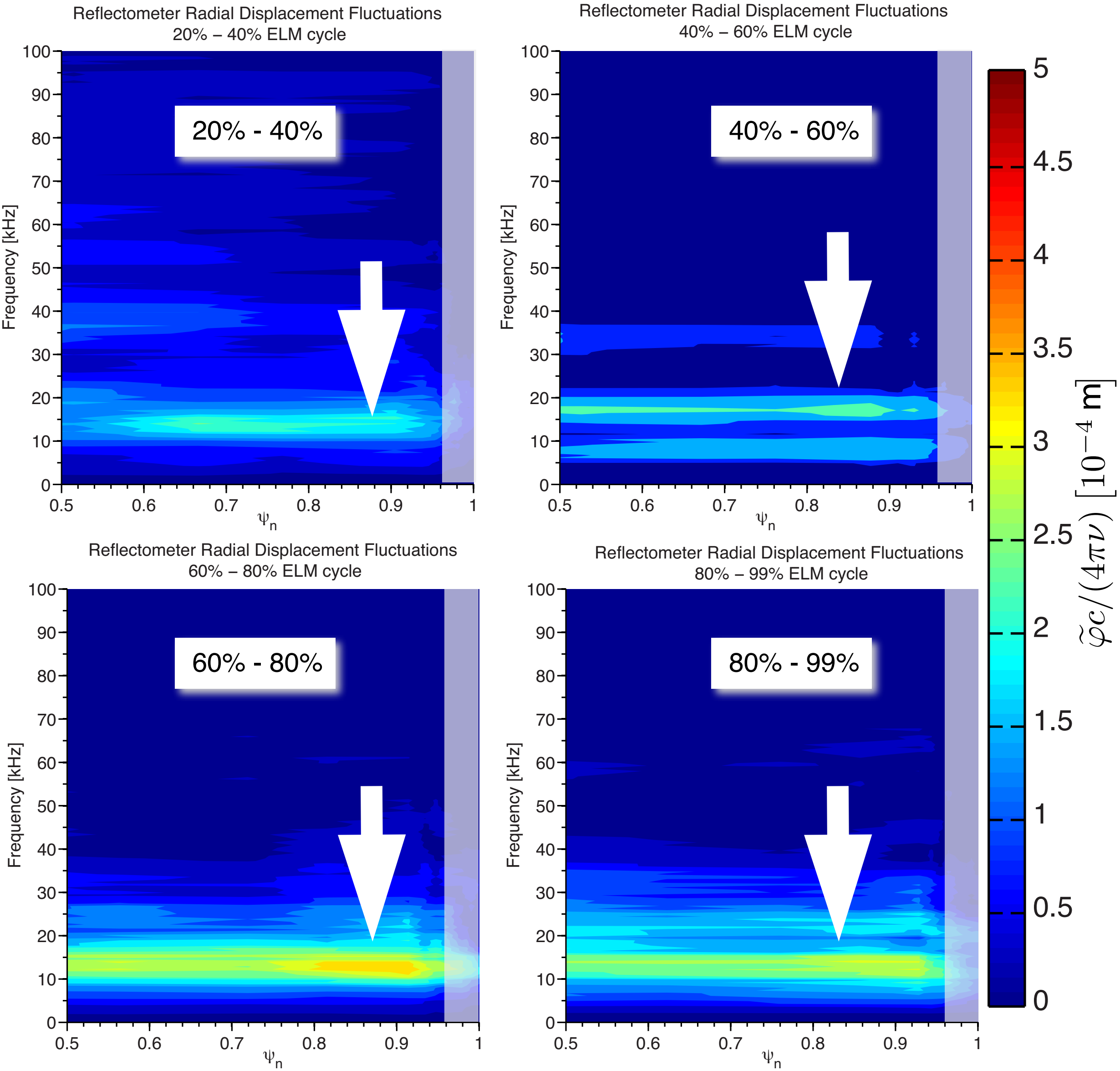

- Radial displacement induced by fluctuations
  - Existence of broadband fluctuations centered around 12 kHz
- Increase of the overall mode amplitude late in ELM cycle
- Caution: Localization of the mode is difficult to assess as it could be due the density scale length

Radial correlation lengths at the pedestal top and steep gradient during the inter-ELM phase

UCLA

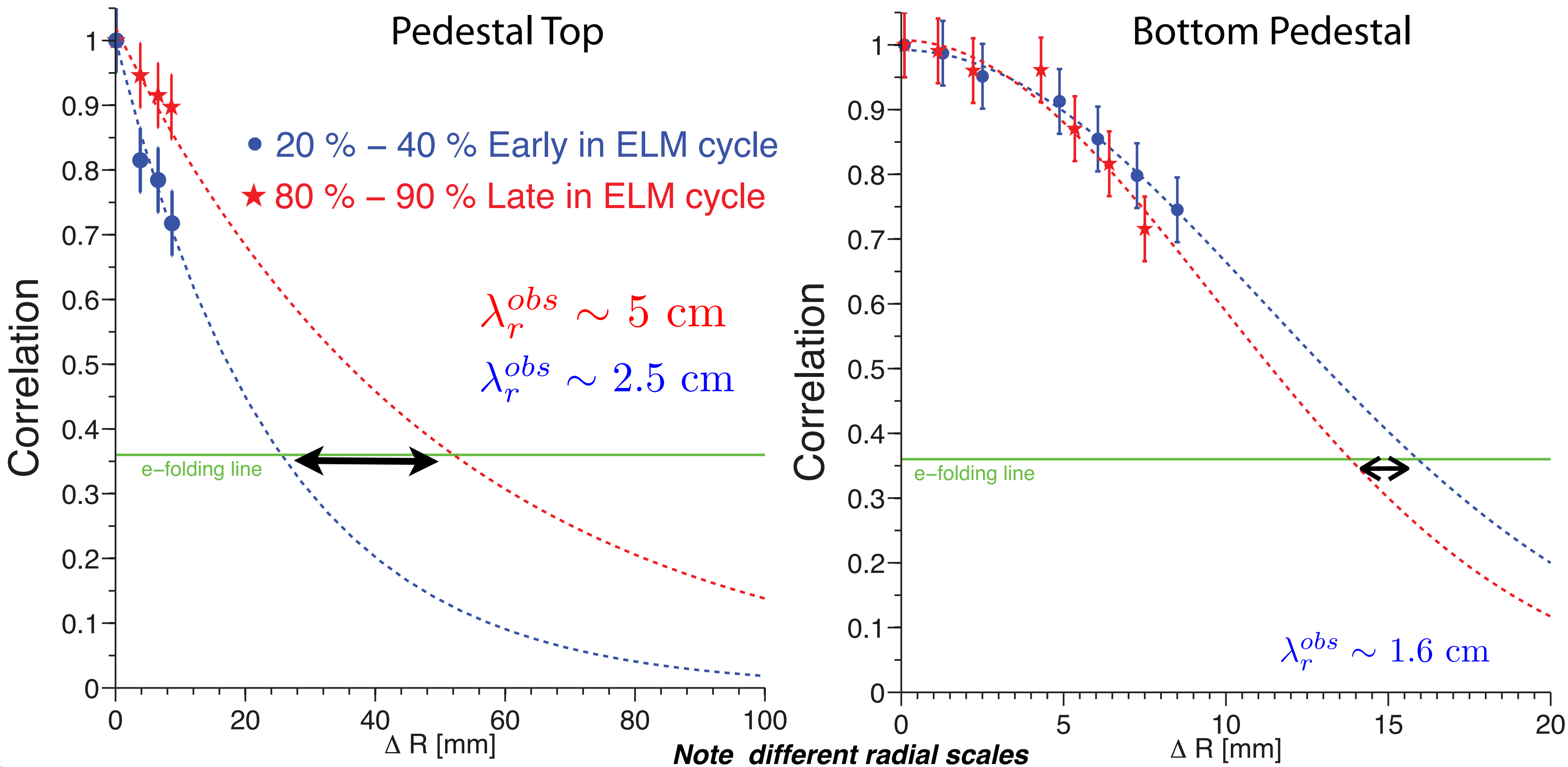

Note different radial scales

- Radial correlation is valuable as it provides the spatial size of a turbulent perturbation (i.e. eddy).
- Pedestal top correlation length is larger than that of the region of steep density gradient

Radial correlation length evolution depends on location inside pedestal region

- Radial correlation length increases at the pedestal top
  - A factor of 2 increase during the last 50% of ELM cycle
  - Presumably due to the increase in radial displacement fluctuations
- Steep gradient correlation length is unchanged
- Quantify the geometric effects on the measured correlation?

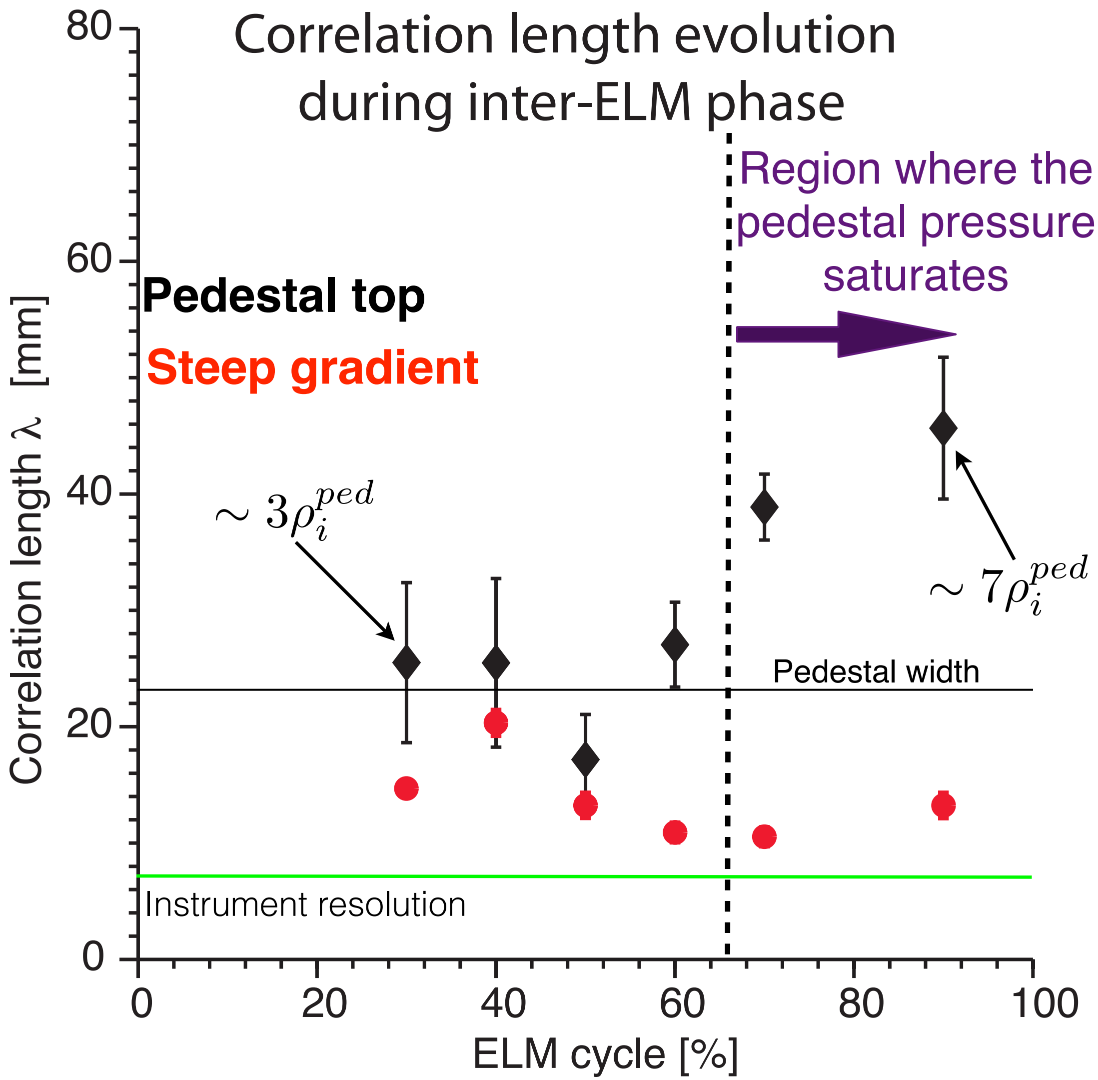

Characterize the pedestal structure evolutions and pedestal turbulence to elucidate the role of transport setting the pedestal structure

- Summary of the Pedestal structure characterization in ELMy H-modes
- Interpretive Transport Analysis
  - SOLPS calculations
  - Comparison with XGC0 - neoclassical simulations
- Fluctuations characterizations during the inter-ELM phase
- Preliminary δf XGC1 calculations and comparison with observations
- Summary/Discussion

Preliminary simulations using XGC1 are performed for cases during the last part of the ELM cycle

- δf mode in XGC1
  - 200 x 60 spatial grid
  - simulation box up to ψ_n ~ 0.95 to include the unstable region
- Collisions and flows are not included in this simulation
- Adiabatic electrons
- Probing the fully nonlinear phase of the simulations
- Full-f simulation in the whole edge with kinetic electrons, flows, and collisions will be performed.

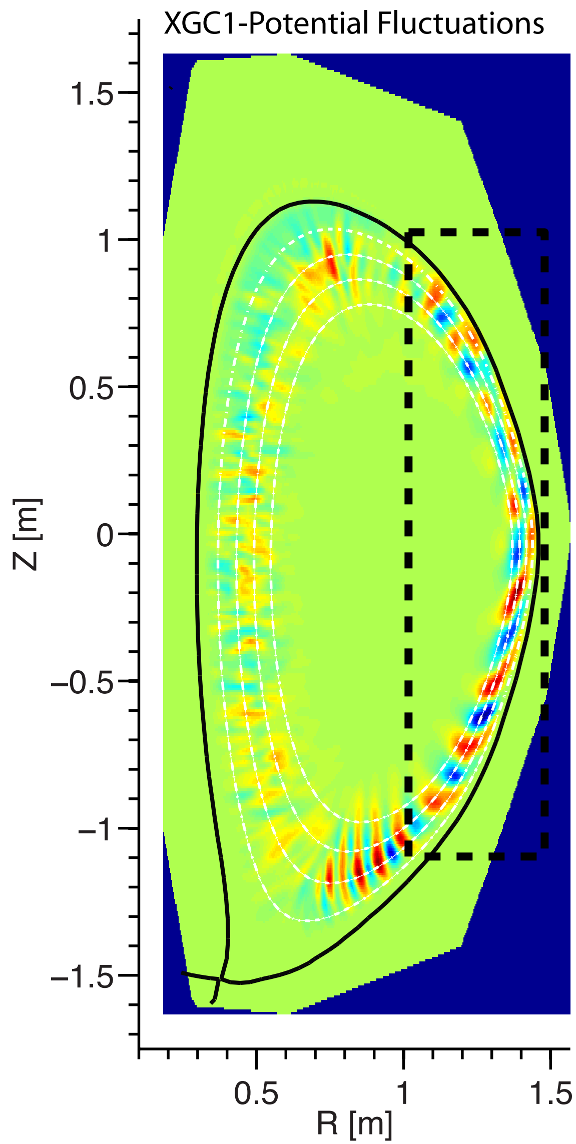

Preliminary simulations using XGC1 are performed for cases during the last part of the ELM cycle

- δf mode in XGC1
  - 200 x 60 spatial grid
  - simulation box up to $\psi_n \sim 0.95$ to include the unstable region
- Collisions and flows are not included in this simulation
- Adiabatic electrons
- Probing the fully nonlinear phase of the simulations
- Full-f simulation in the whole edge with kinetic electrons, flows, and collisions will be performed.

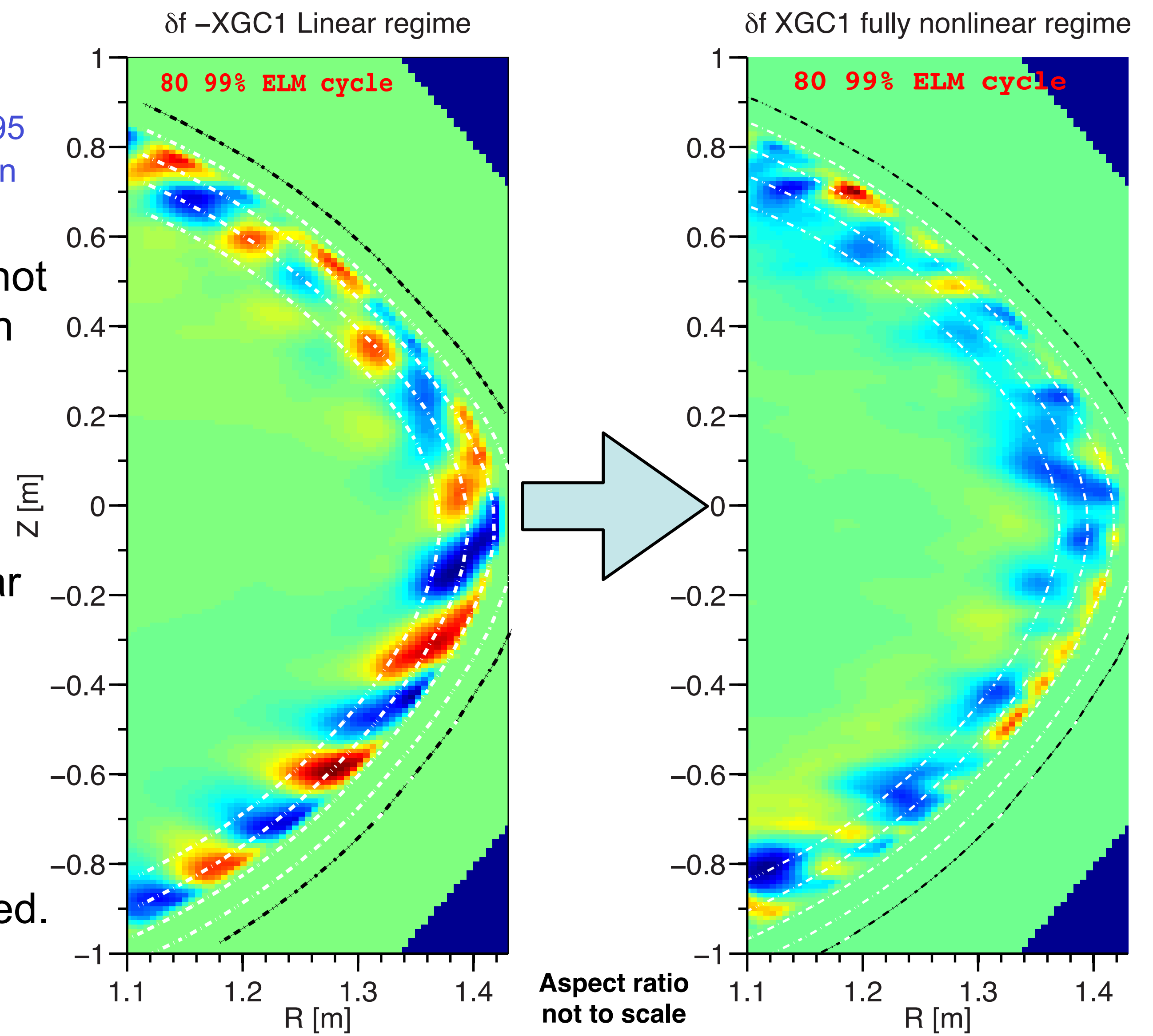

Preliminary simulations from XGC1 show localized fluctuations with experimental level radial and poloidal correlation lengths

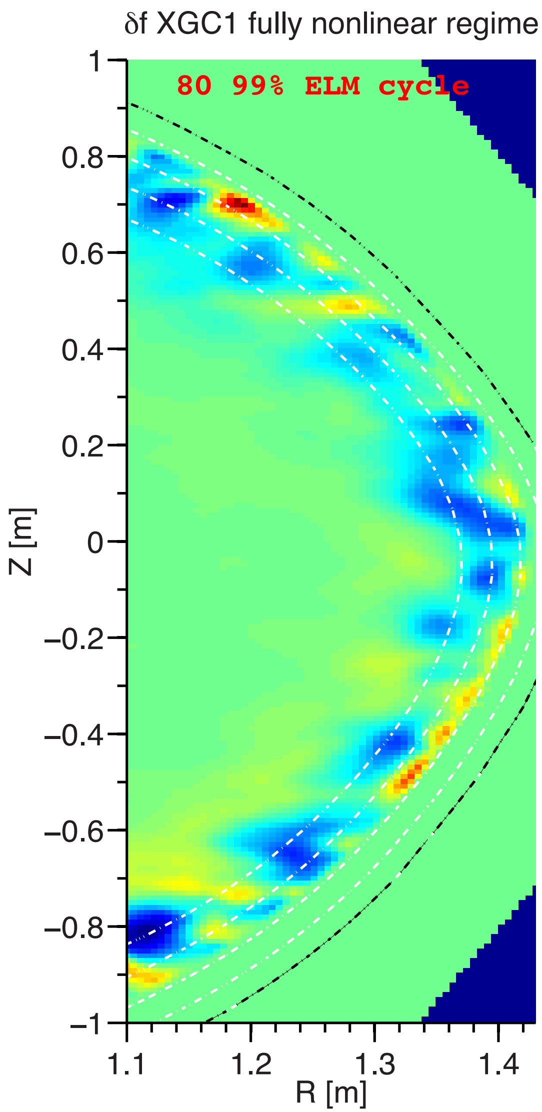

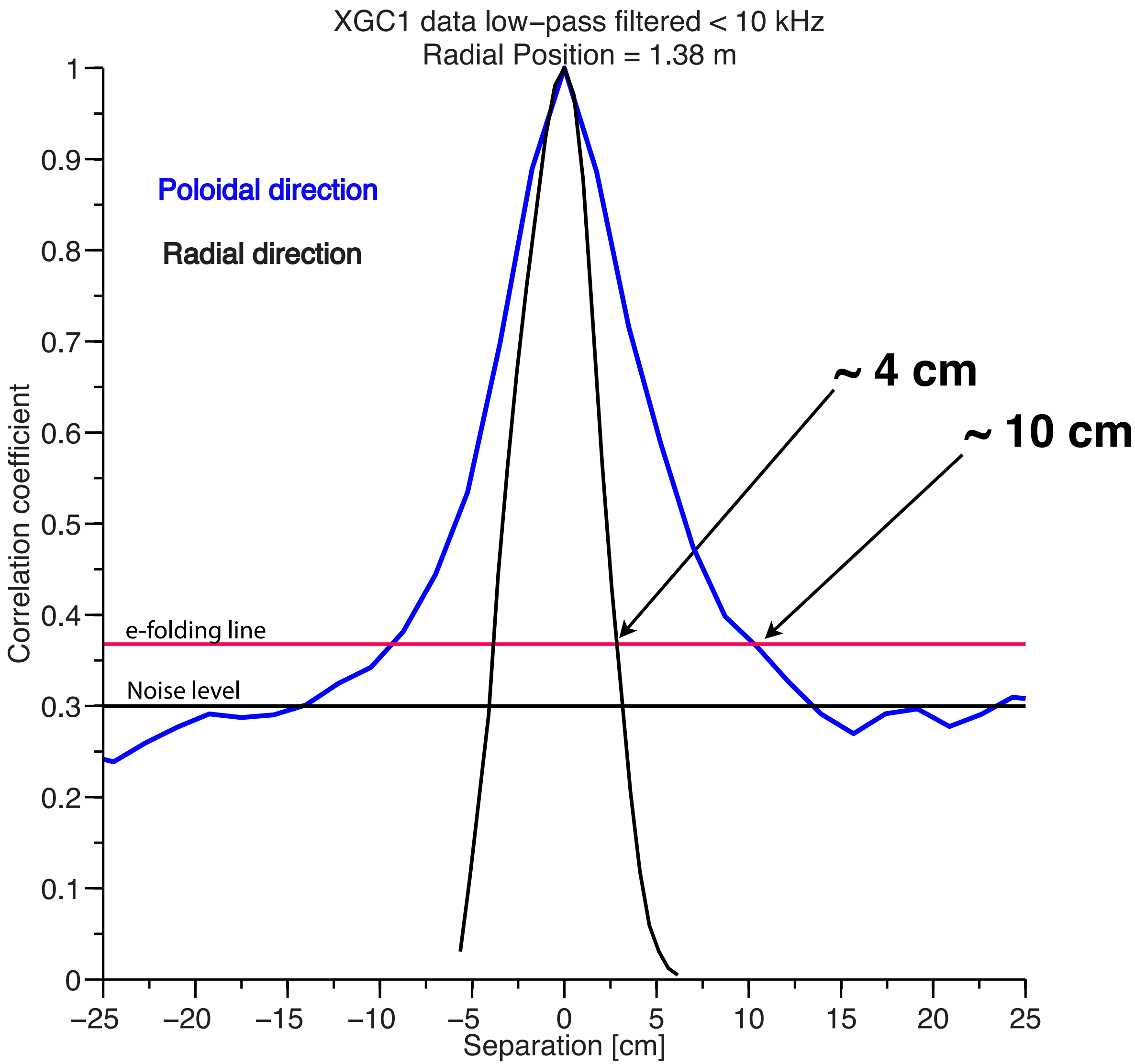

Summary (I)

- Using ELMy discharges, we observed during the ELM cycle:
  - Continuous increase of the electron temperature and much less variation in electron density and pressure build up and at time saturation prior to the ELM onset
  - Consistent with barrier expansion phenomenology observed in other tokamaks
  - Pressure gradient, however, is clamped during most of the ELM cycle
- Interpretive transport analysis using SOLPS, and XGC1
  - No convincing correlation between the electron heat flux and ELM cycle
  - Ion heat flux is larger in the pedestal region late in the ELM cycle
    - In addition, Ion heat flux larger than neoclassical estimates from XGC0
  - Particle flux throughout remains difficult to assess

Summary (II)

- Characterization of the fluctuations during the inter-ELM phase
  - BES and reflectometry confirm ion scale turbulence $0.2 \leq k_{\perp}\rho_i \leq 0.7$
  - Poloidal correlation is larger than radial correlation length
- Preliminary simulations with XGC1 are performed
  - Used in δf mode in XGC1
  - Thus far, simulation results correlation lengths measurements agree with experimental observations
    - » Most unstable mode is ITG in simulation: identification of turbulence in experiment, however, will require full-f XGC1.
    - » Addition of electrons and flows will give a better sense of the heat transport responsible for clamping the pedestal gradient
- More work: A continuation and expansion of these comparisons to simulations with the ultimate goal of identification of types of turbulence
  - Further 3D analysis of reflectometry are underway to verify the 2D approximation initially performed
    - How well the diagnostic determine the true radial correlation length
  - Extend the simulation to full-f mode using XGC1 and account for measured flows and add collision.

Backup

Using TRANSP, no significant change in the electron heat diffusivity at the pedestal prior to the onset of ELM

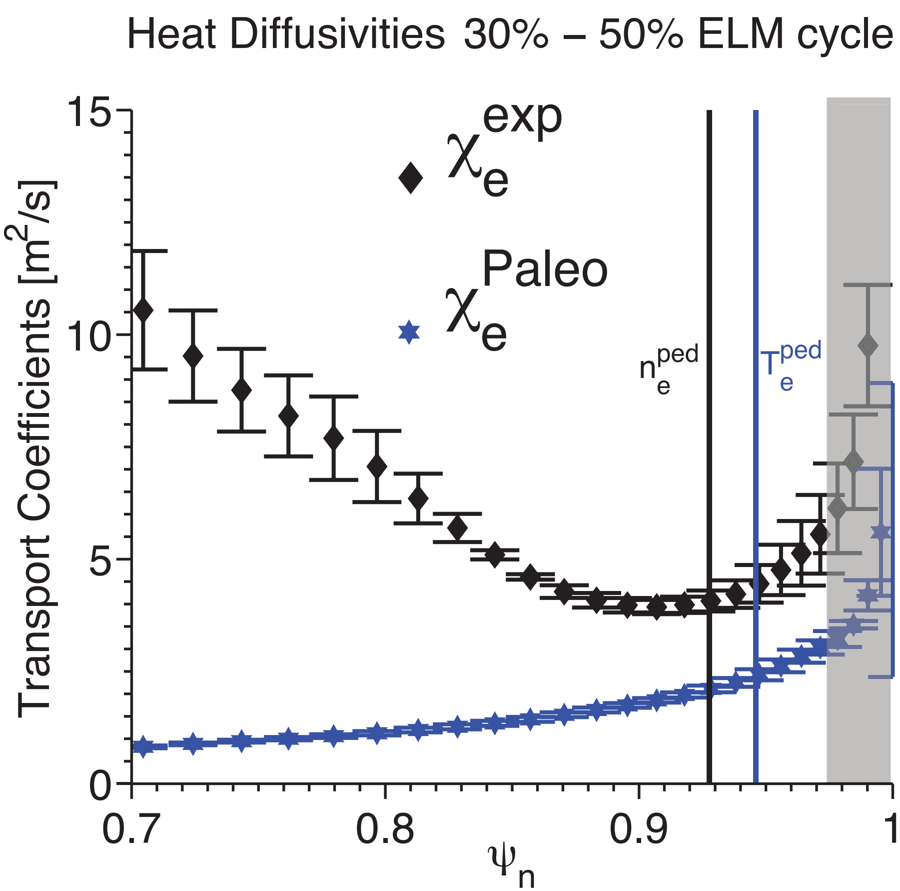

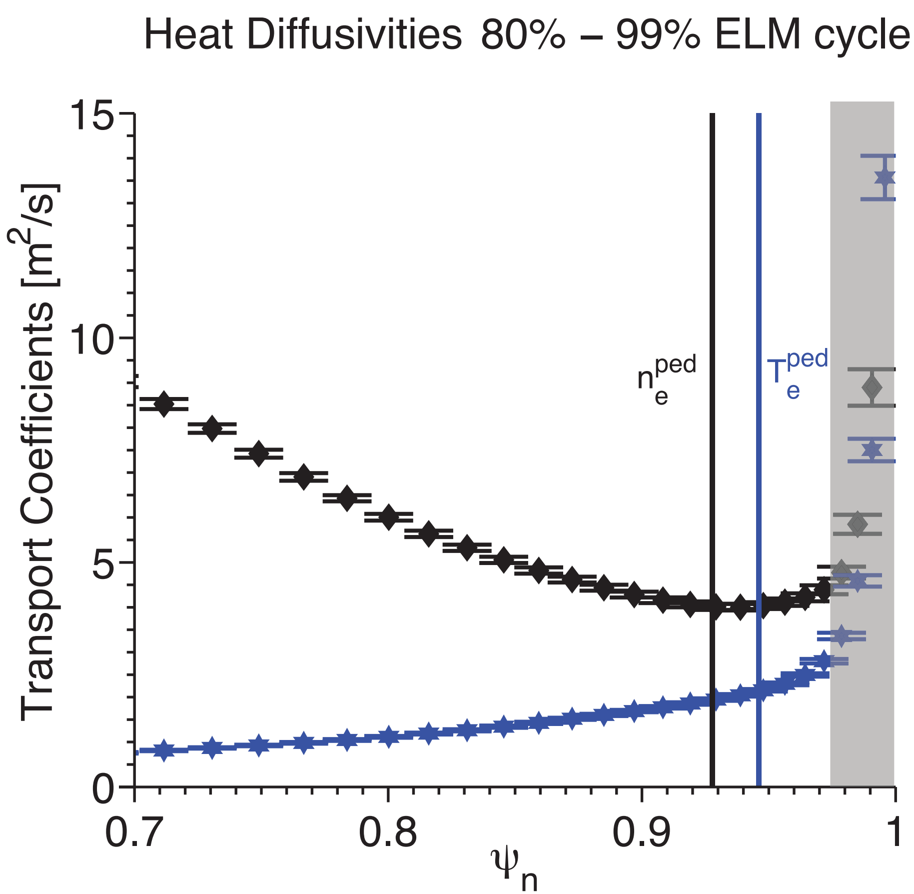

- Bottom half of the pedestal suggests that paleoclassical transport could be a major contributor to the electron heat transport, but not at the pedestal top.
- In the pedestal top, neoclassical heat diffusivities appear to overestimate the experimental ion χ .

Using TRANSP, no significant change in the electron heat diffusivity at the pedestal prior to the onset of ELM

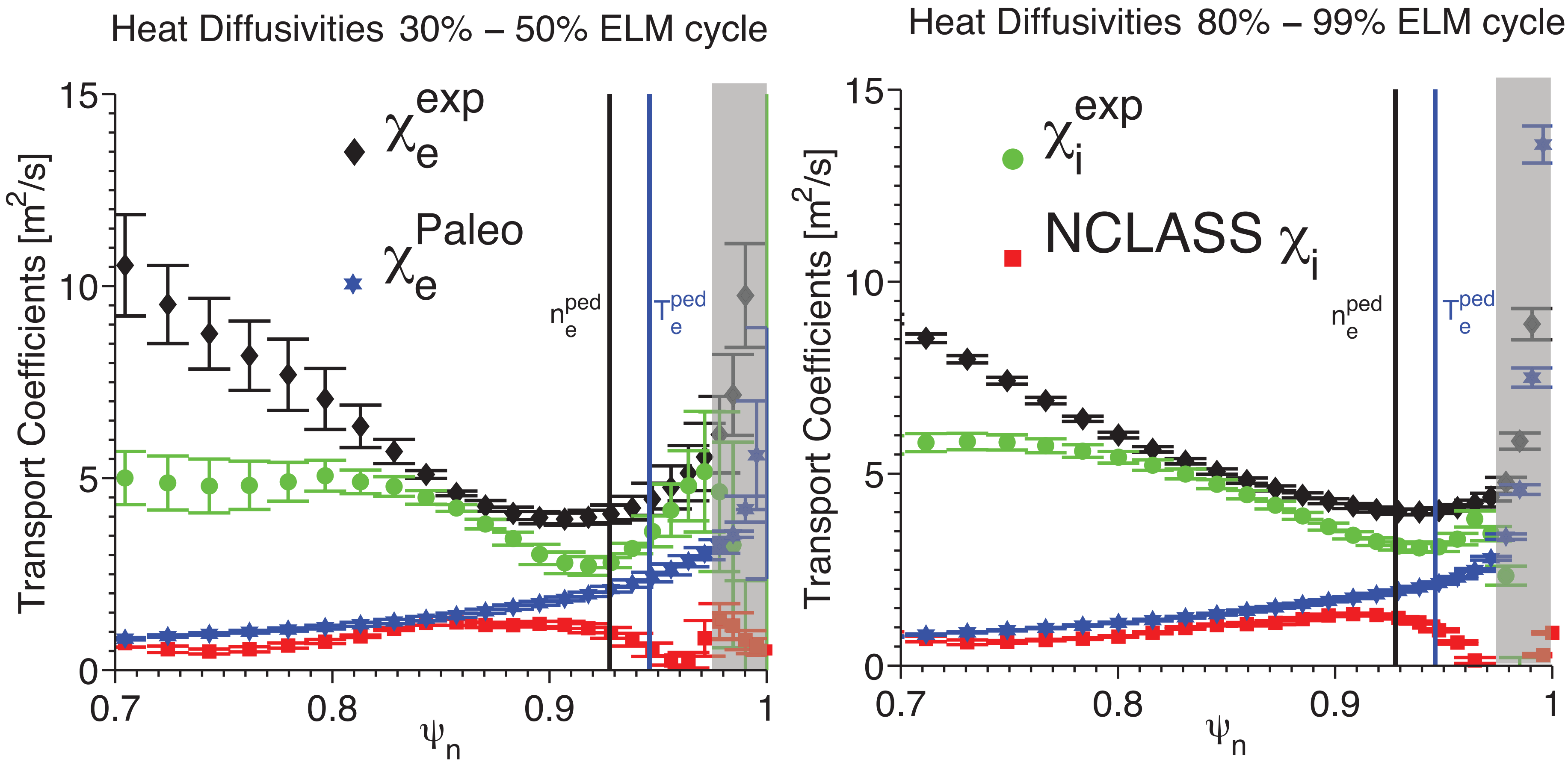

- Bottom half of the pedestal suggests that paleoclassical transport could be a major contributor to the electron heat transport, but not at the pedestal top.
- In the pedestal top, neoclassical heat diffusivities appear to overestimate the experimental ion χ .

The trends during the inter-ELM phase in heat diffusivities are difficult to unravel

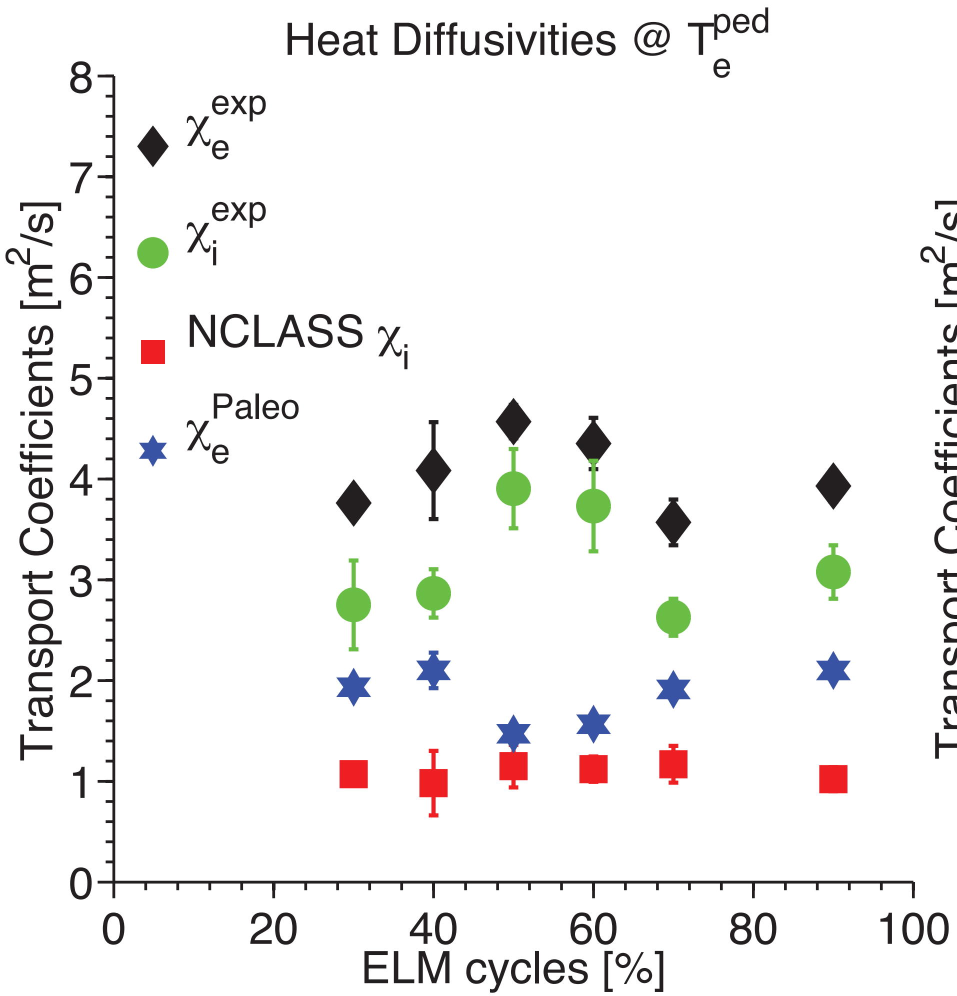

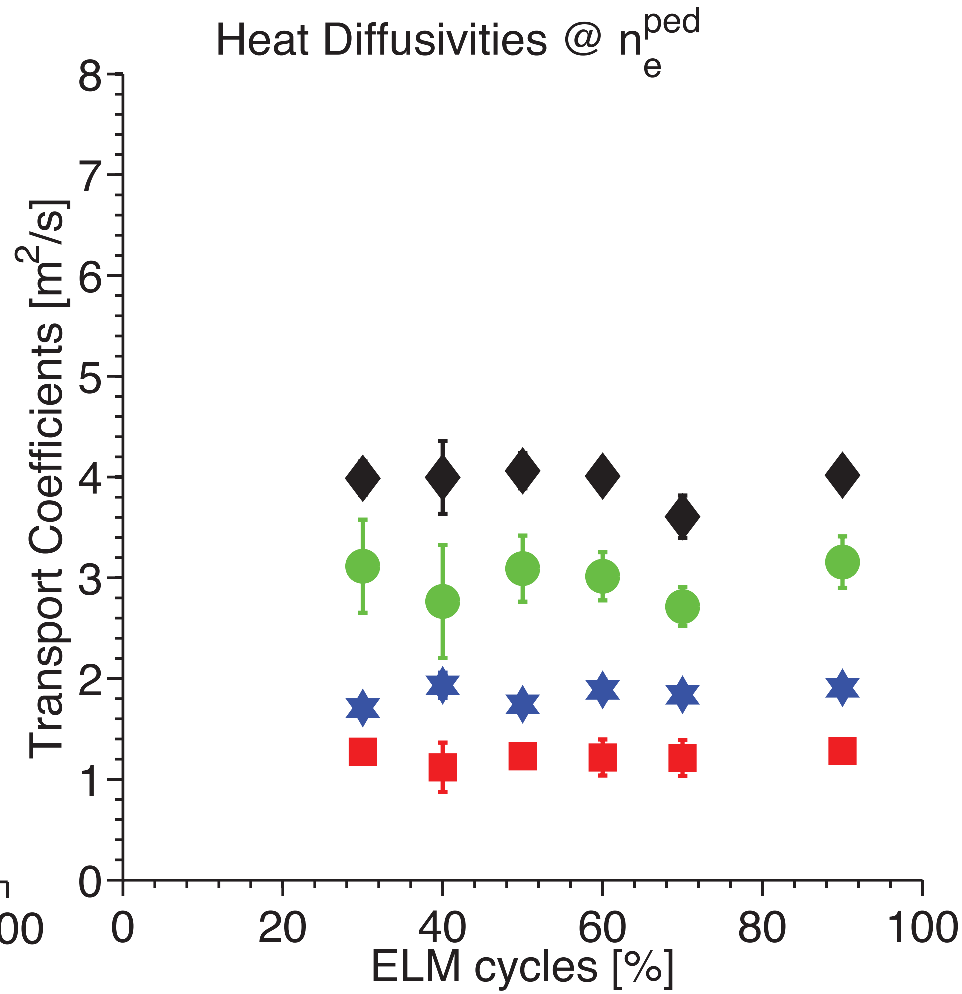

Using both BES and correlation reflectometry, the inter-ELM spatial structure of fluctuations exhibit ion-scale microturbulence

- Strong anisotropy of the turbulence is observed during the inter-ELM phase
- Turbulence data suggests microturbulence with $0.2 \leq k_\perp \rho_i \leq 0.7$ propagating in ion diamagnetic direction

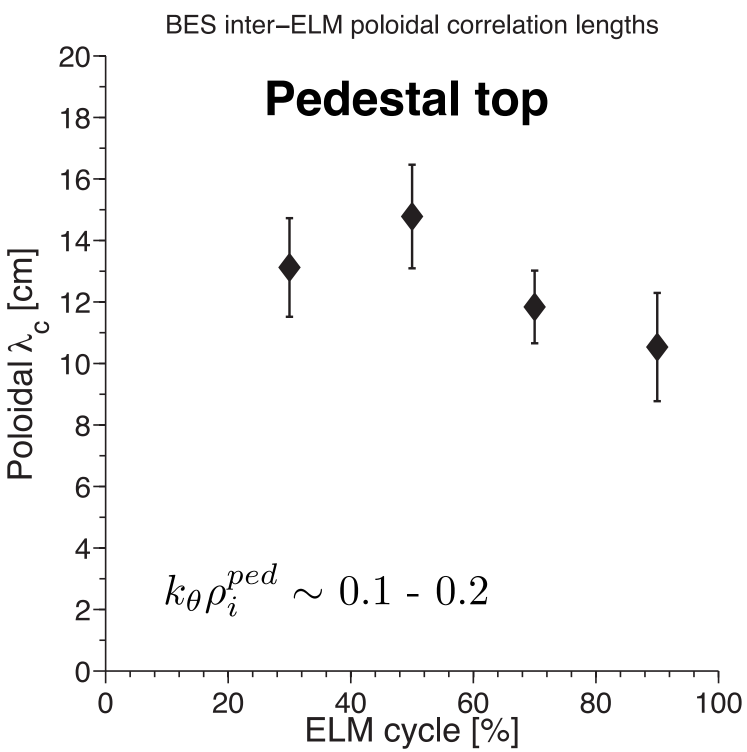

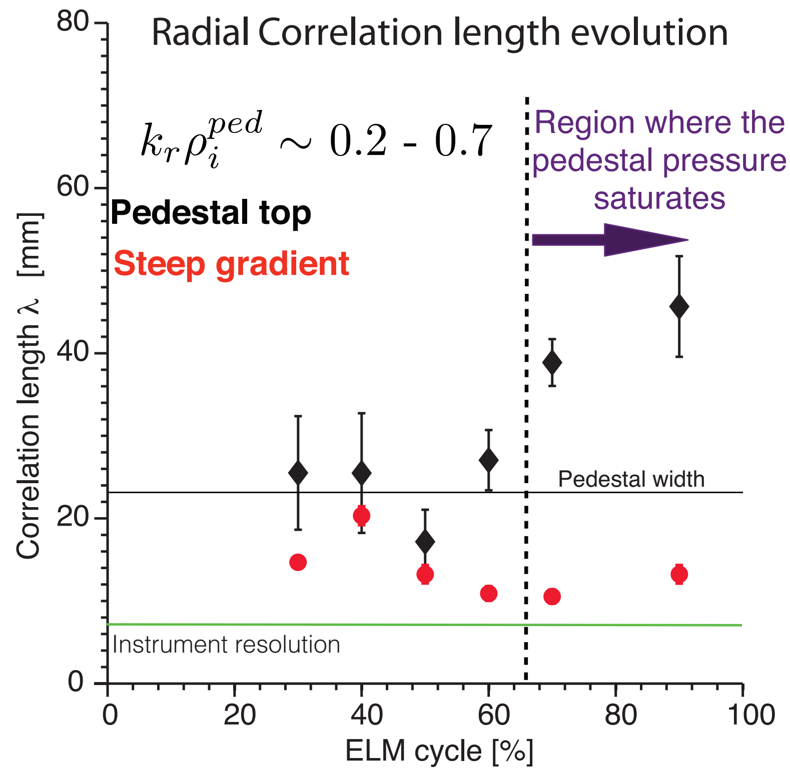

Apparent correlation between the magnetic shear at the pedestal top and fluctuations amplitude increase during the ELM cycle

$S = q\partial_r q$ parameter during ELM cycle

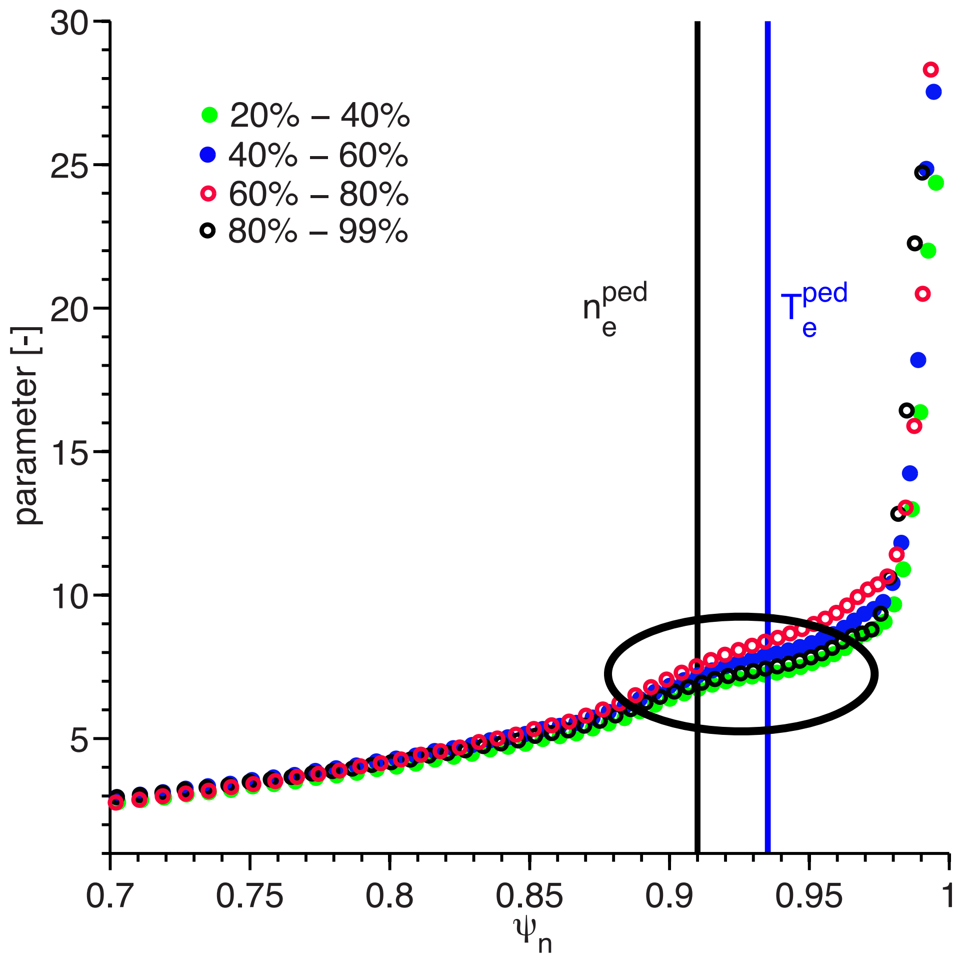

Radial averaging of displacement fluctuation spectra

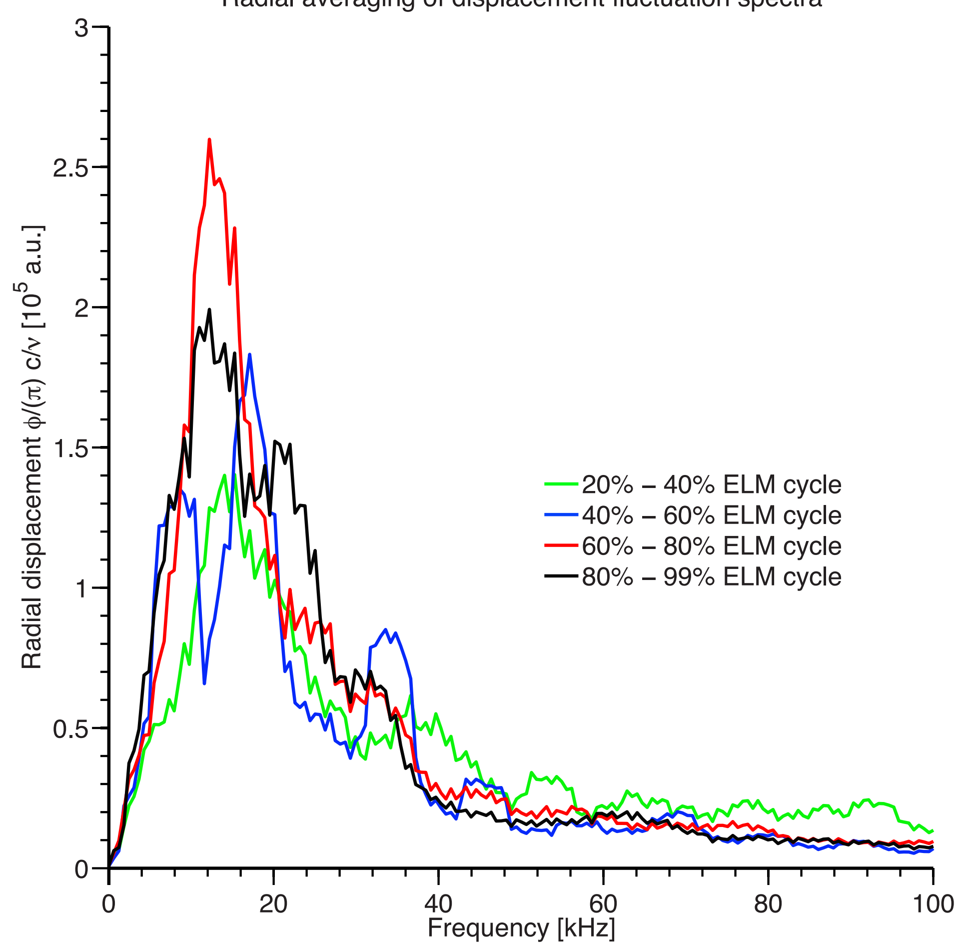

ITG drives peaks at the pedestal top and R/L_{Ti} is larger than R/L_{Ti_crit}

ITG drive during inter-ELM phase

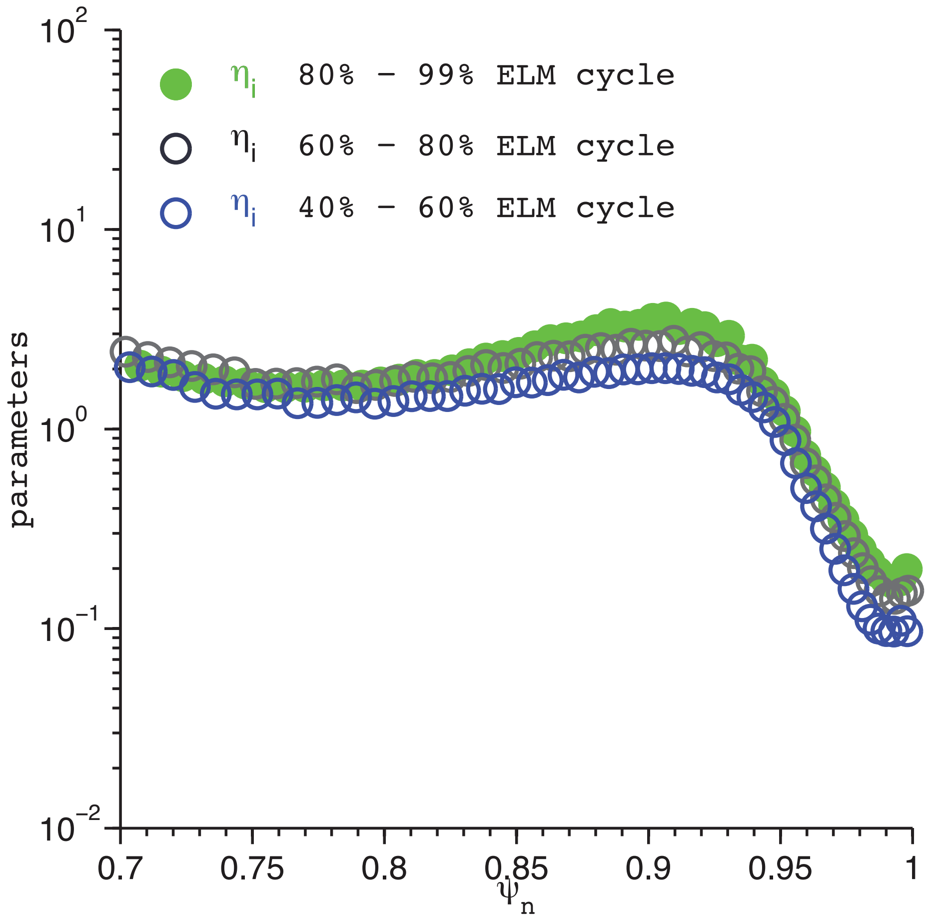

Critical ITG Gradient

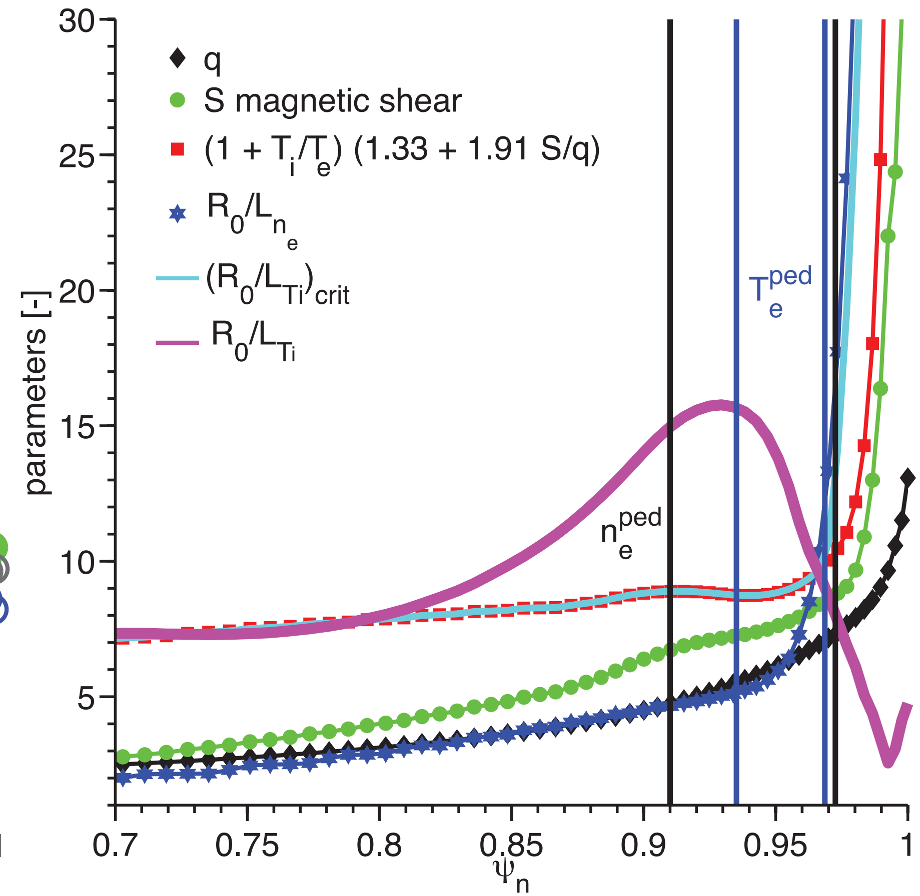

- Jenko's approximation suggests ITG could be unstable in the pedestal top.

2-D interpretive modeling with SOLPS*

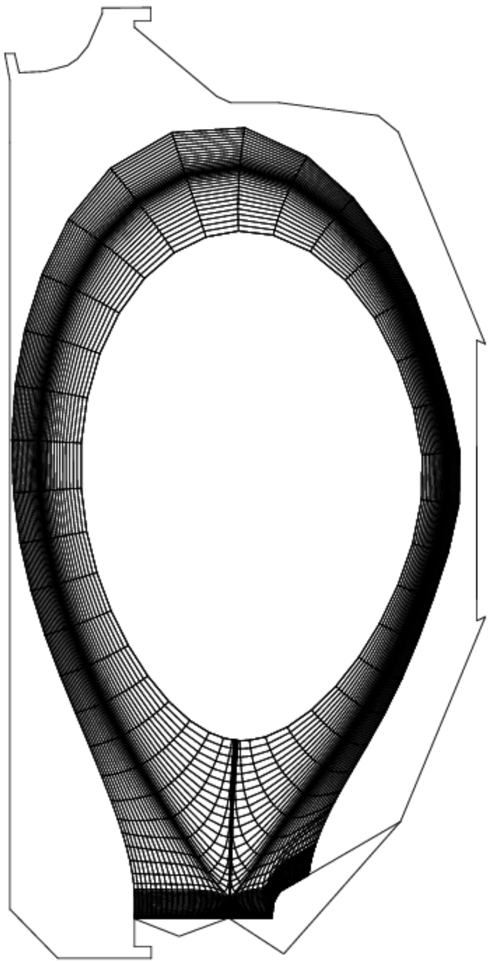

- Solves conservation equations for
  – Density, parallel momentum of each charge state, electron energy, ion energy, charge
- Includes models for plasma transport
  – Parallel: classical along field lines
    - with particle and heat fluxes limited to simulate kinetic effects
  – Radial: D, χ adjusted to fit measured plasma density and temperature profiles.
  – ExB and grad B drift effects not yet included.
  – Neutral transport: Kinetic, using the Eirene Monte Carlo code
- Yields edge transport coefficients, self-consistent neutral fueling profiles

*R. Schneider et al, Contrib. Plasma Phys. 46 (2006) 3.

Pedestal pressure height increases with shaping (triangularity δ)

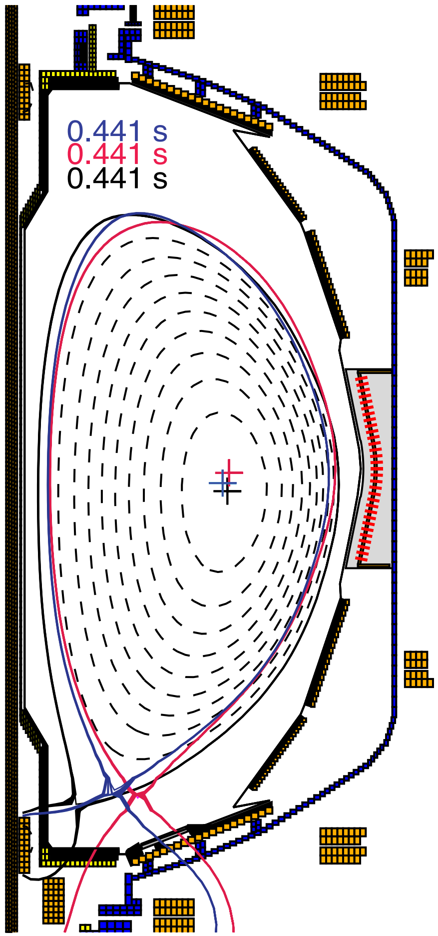

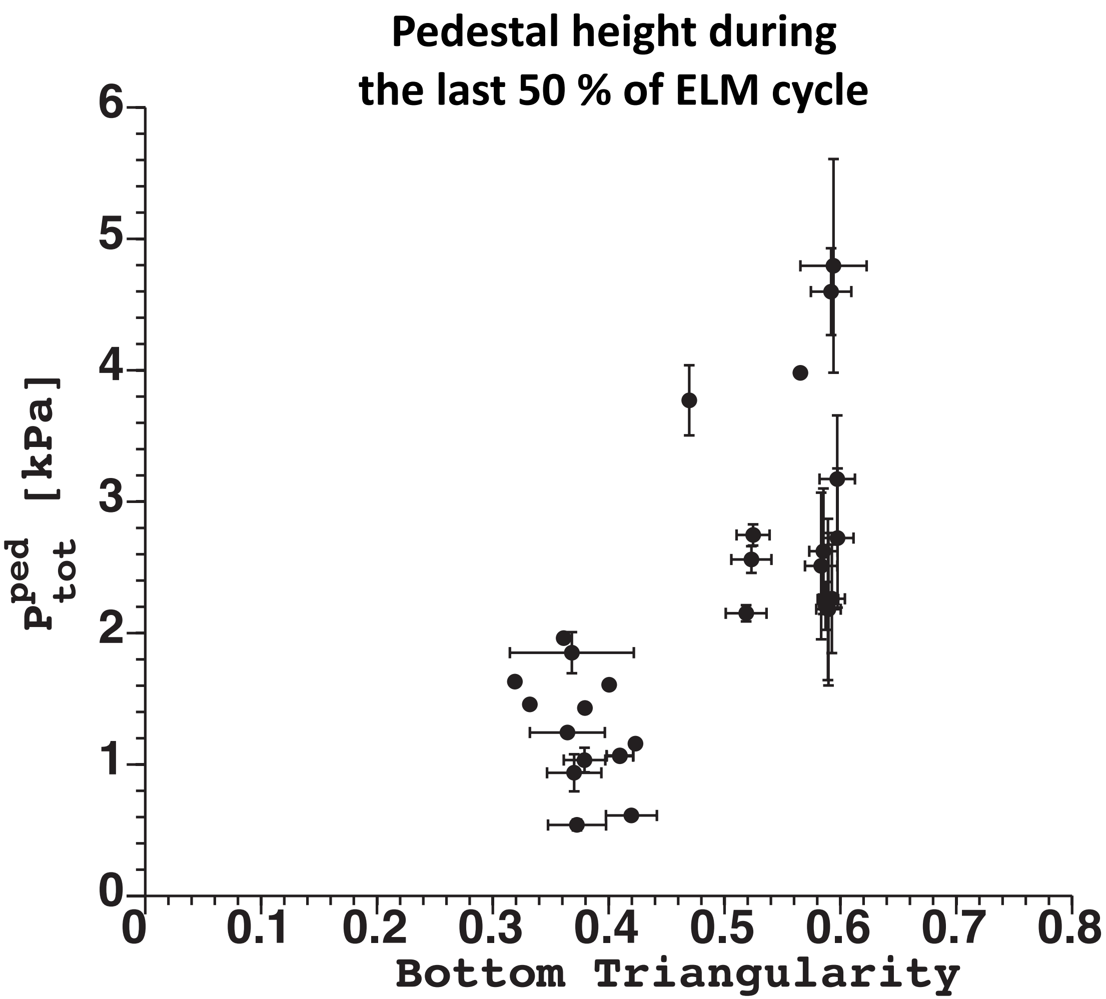

Increasing shaping leads to stability limits at higher P'_{ped}

Stability diagram with and without lithium: Lithium cases are farther away from the kink/peeling boundary

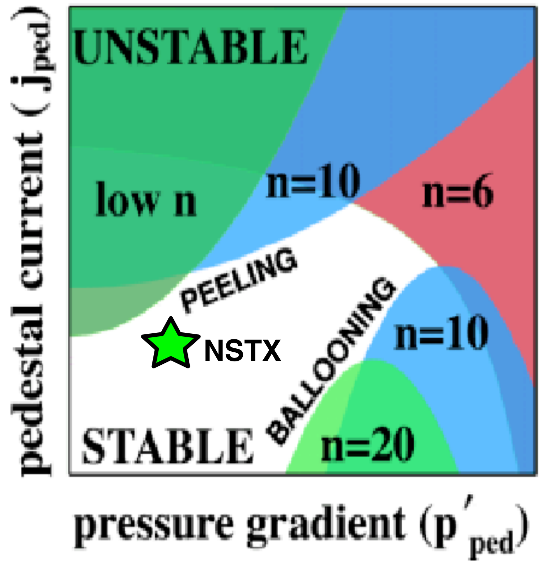

Stability diagram with and without lithium: Lithium cases are farther away from the kink/peeling boundary

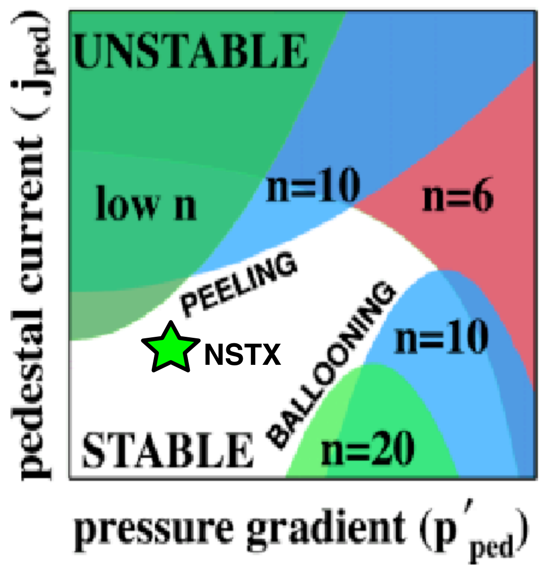

Consistent with NSTX close to the kink/peeling stability boundary

Lithium coatings are a useful tool for shifting peak pressure gradient inward and stabilizing kink/peeling modes.

Stability diagram with and without lithium: Lithium cases are farther away from the kink/peeling boundary

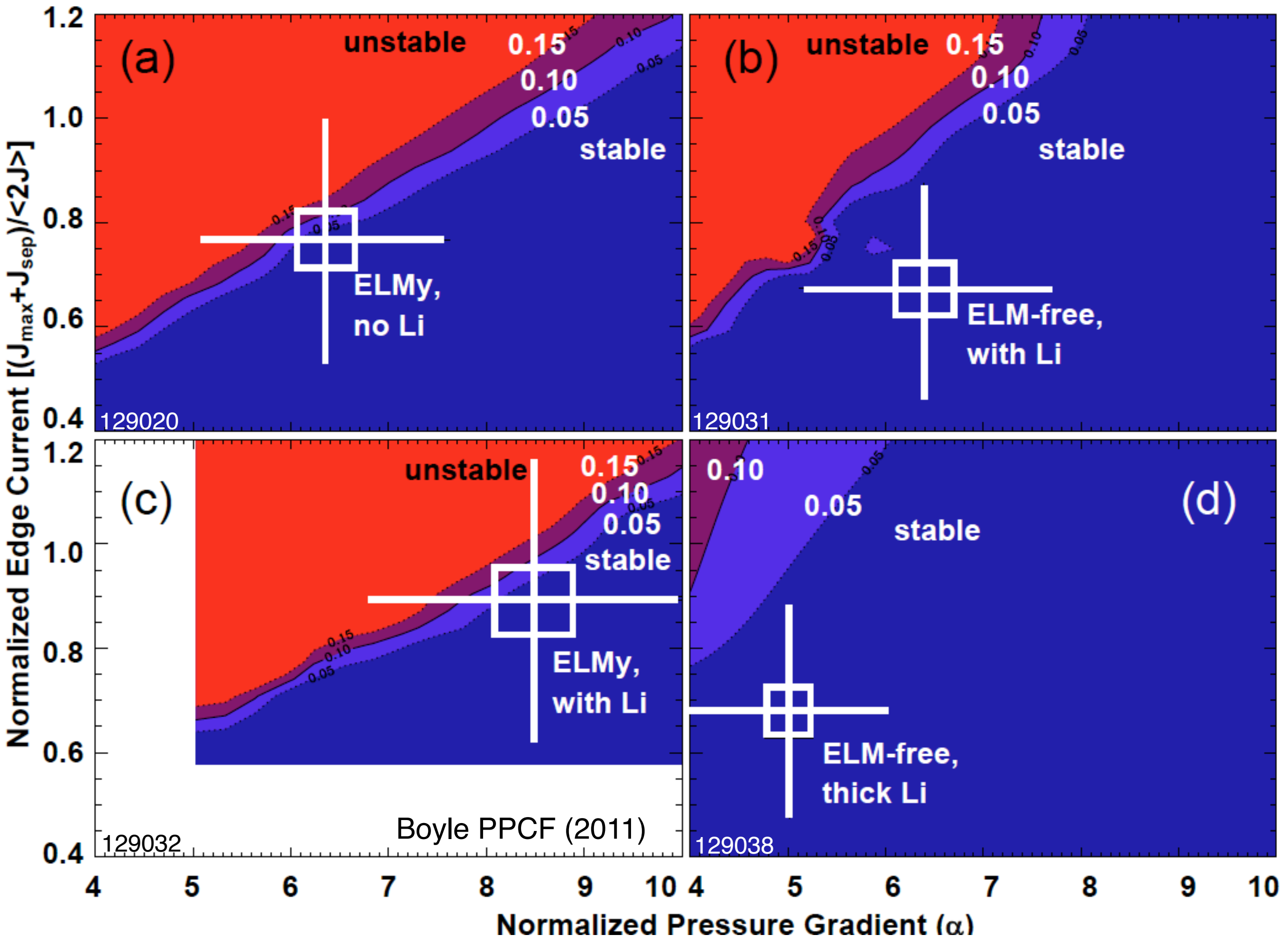

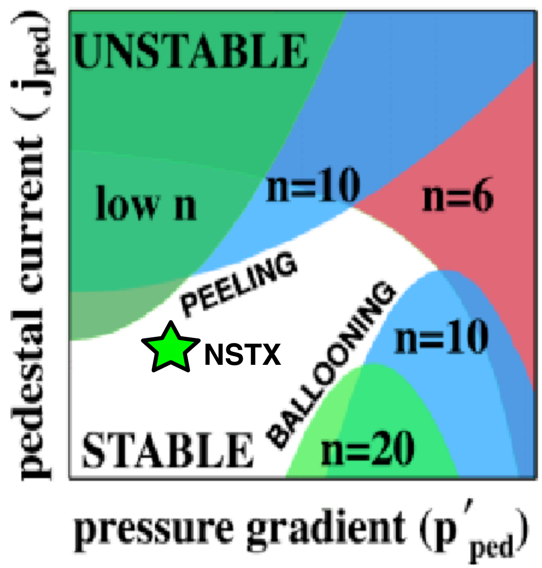

Consistent with NSTX close to the kink/peeling stability boundary

Lithium coatings are a useful tool for shifting peak pressure gradient inward and stabilizing kink/peeling modes.

Role of the edge density fluctuations on setting the pedestal structure during the inter-ELM phase

- Pedestal gradient has been predicted to be constrained by the onset of kinetic ballooning mode (KBM)* *Snyder PoP 9 (2002)
  - Recent DIIID work has shown observations of modes localized in the pedestal region with features similar to KBM Yan PRL 107 (2011)
  - KBM characterized by:
    - $k_\perp \rho_i < 1$
    - modes have radial scales of the order few cm in the pedestal region of NSTX
    - fast rising growth rate increasing with electron β
    - propagation in the ion diamagnetic direction.

- NSTX: We look for evidence of pedestal-localized microinstabilities, and their correlation with the ELM cycle
  - Use both reflectometry and BES
  - Because it's hard to conclusively identify KBM, we characterize our instabilities in terms of radial scale, wave number, and propagation direction

Turbulent fluctuations during the inter-ELM dynamics determined using the correlation reflectometry (UCLA)

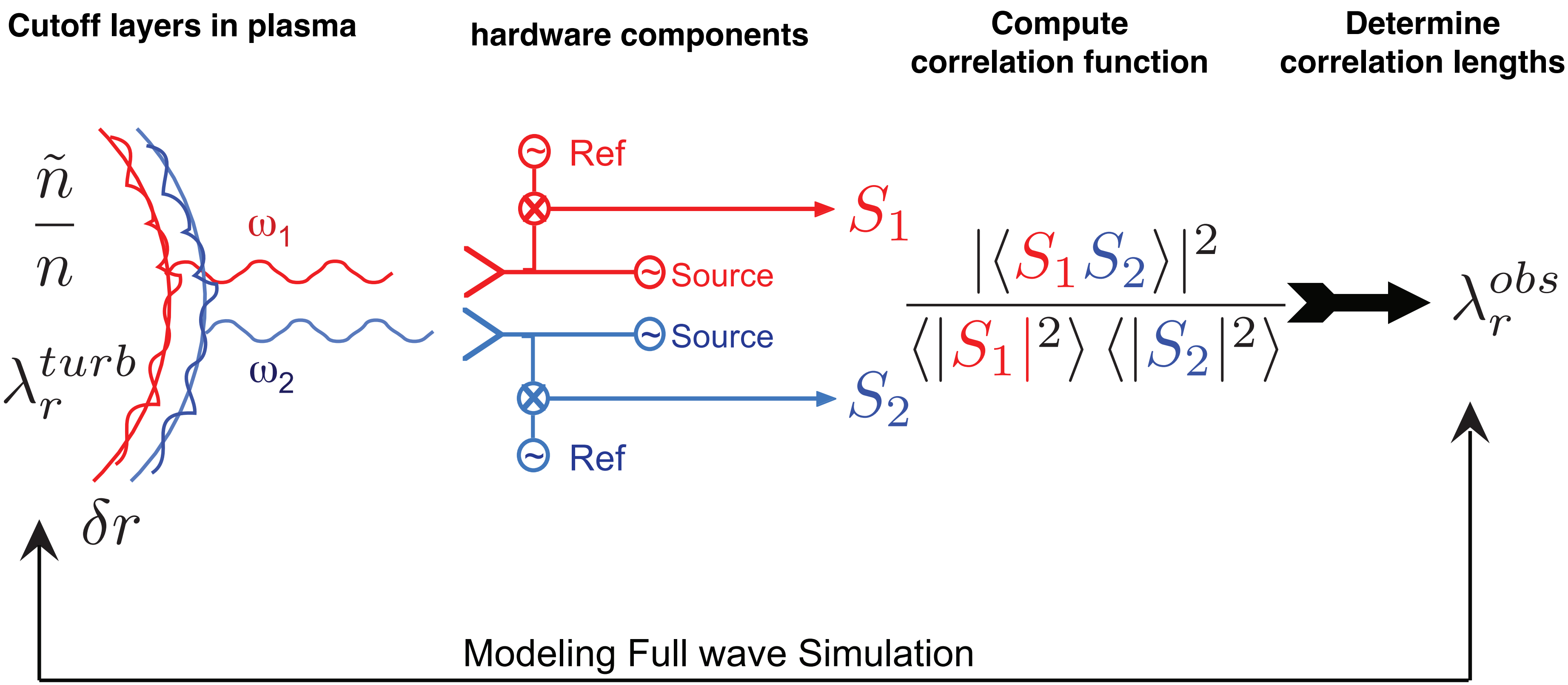

- Compare the correlation length measurements with 2D full wave simulations to remove potential instrument function $\lambda_r^{turb} \neq \lambda_r^{obs}$
  - density fluctuation level, equilibrium profiles, and turbulent correlation lengths.

Radial density correlation lengths at the pedestal top and steep gradient region

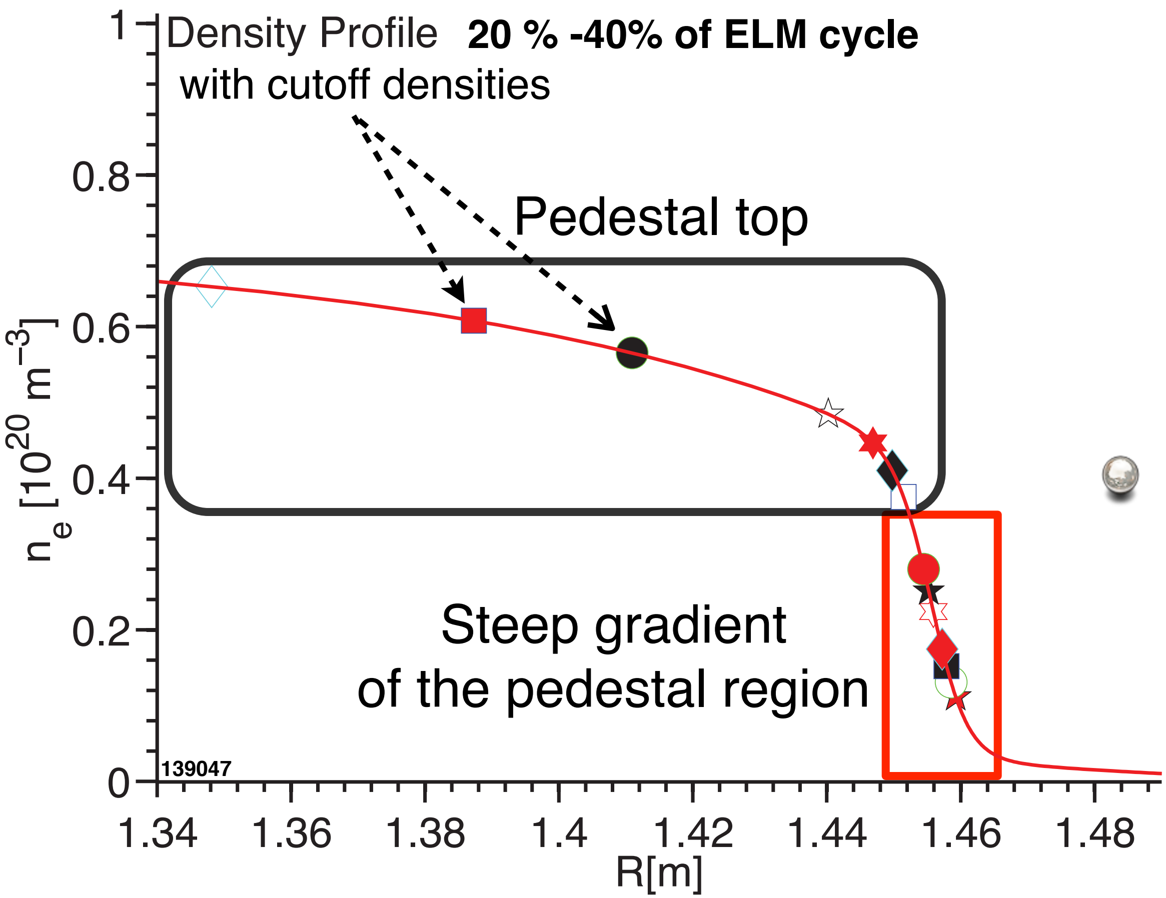

- The density fluctuations are measured using a 16-channel O-mode reflectometer

Crocker, PPCF (2011)

- Using two-point correlation the radial correlation function is determined.
  - tracks the equilibrium plasma motion

2D full wave modeling (FWR2D*) provides correspondence between observed quantities and turbulent parameters

*Valeo, PPCF (2002)

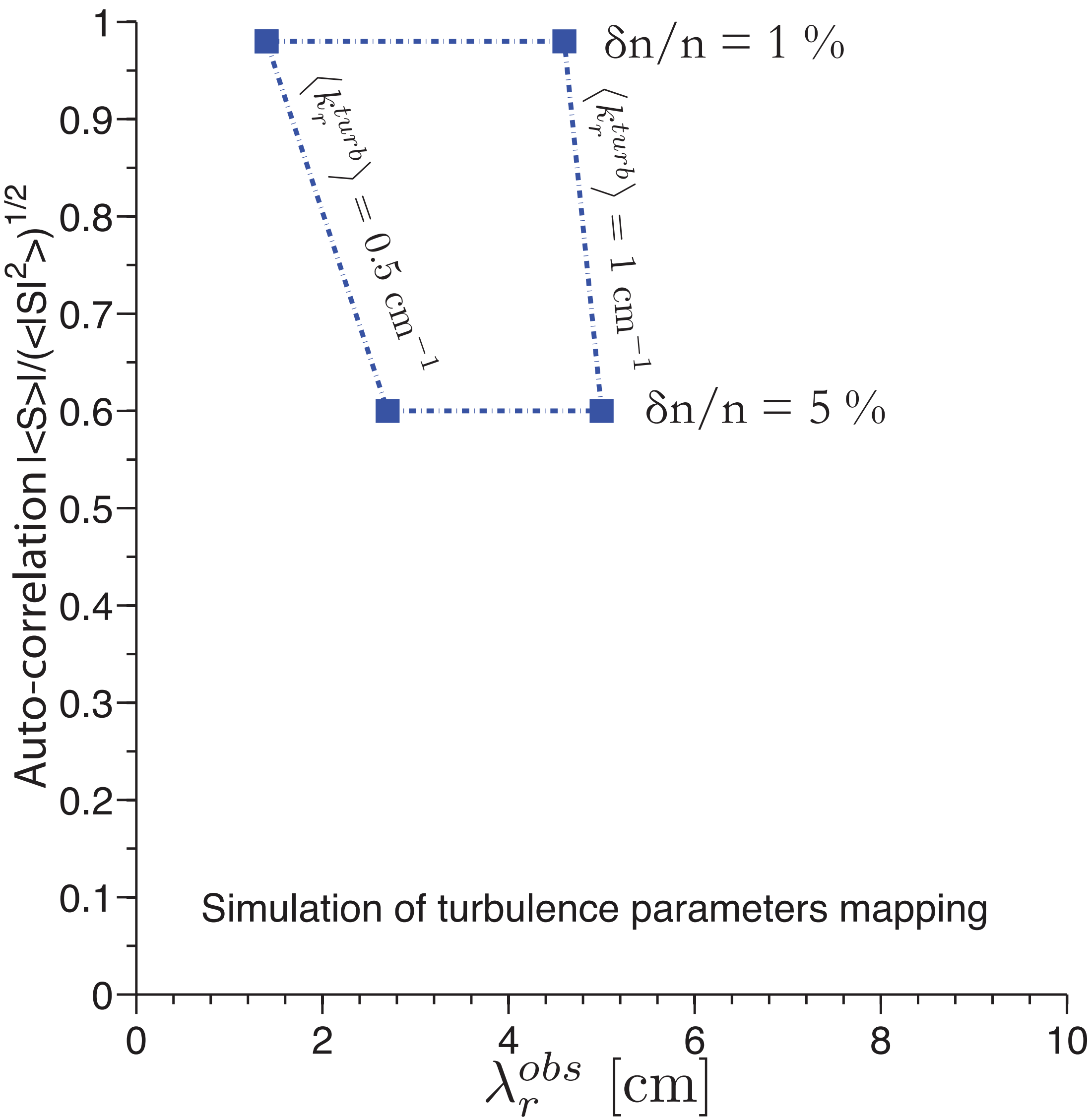

- Density fluctuations are generated using a model based gaussian distribution

Kramer RSI 74 (2003)

$$\left(\frac{\delta n}{n}\right)^2 e^{-\delta R^2/\lambda_{turb}^2}$$

2D full wave simulation of correlation function inside pedestal region reproduces measurements

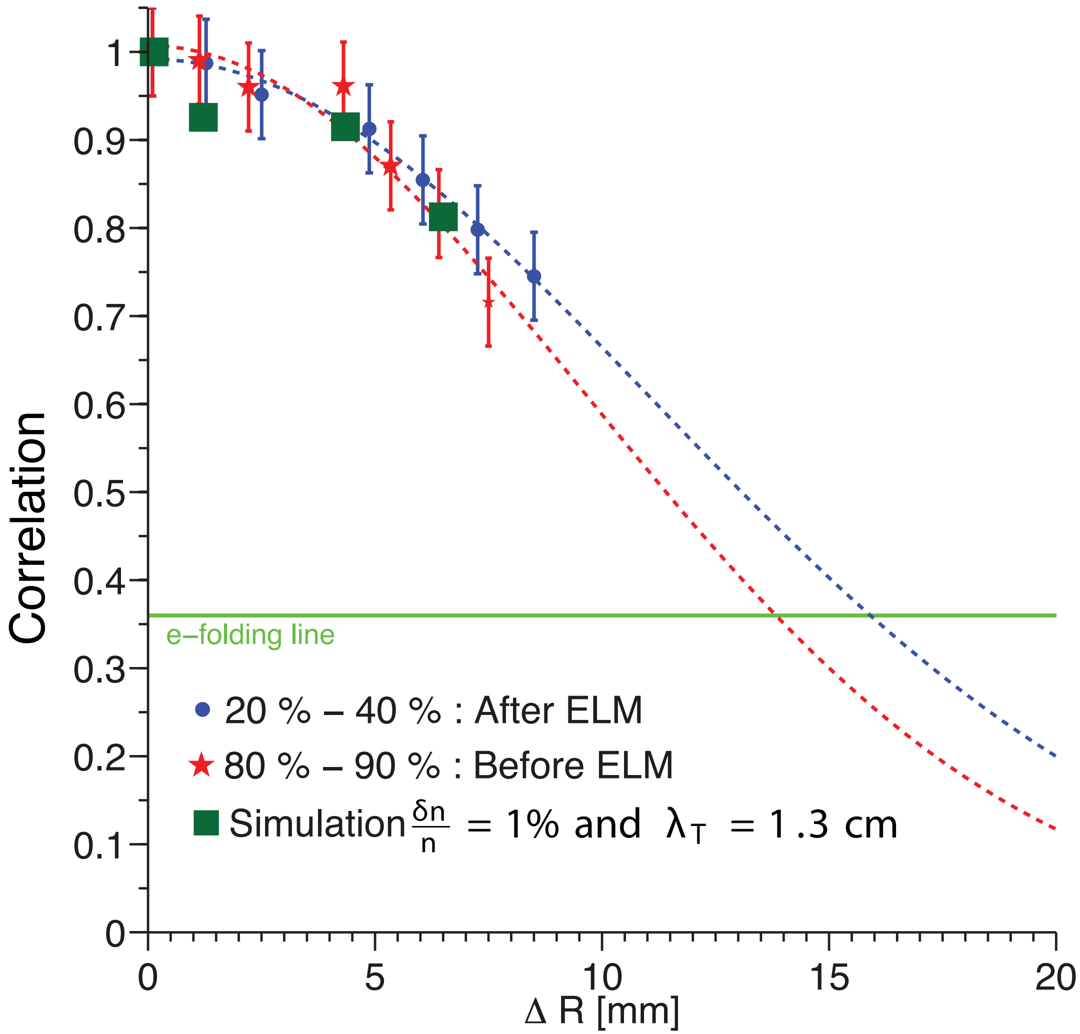

Observed correlation length corresponds to an average eddy size of ~ 1.3 cm with fluctuation level in the vicinity of 1% in the gradient region.